CrossMark

ORIGINAL ARTICLE

Characterization of photosynthetic acclimation in *Phoenix dactylifera* by a modified Arrhenius equation originally developed for leaf respiration

Jörg Kruse[1] · Mark A. Adams[2] · Georgi Kadinov[1] · Leila Arab[1] · Jürgen Kreuzwieser[1] ·
Saleh Alfarraj[3] · Waltraud Schulze[4] · Heinz Rennenberg[1,3]

Abstract

Key message **Instantaneous temperature responses of leaf respiration and photosynthesis can be described by the same equation, to help understand acclimation of primary metabolism to altered growth temperature and water supply.**

Abstract We used a three-parameter, modified Arrhenius equation, originally developed for leaf respiration, to characterize A/T curves of Date Palm and acclimation to elevated growth temperature and water deprivation:

$$A_{\mathrm{T}} = A_{\mathrm{ref}} \times e^{\left[\frac{E_{\mathrm{o}}(\mathrm{Ref}_A)}{\Re} \times \left(\frac{T - T_{\mathrm{ref}}}{T \times T_{\mathrm{ref}}} \right) + \delta_A \times \left(\frac{T - T_{\mathrm{ref}}}{T \times T_{\mathrm{ref}}} \right)^2 \right]}$$

where A_{ref} is the net CO_2-assimilation (A) at fixed reference temperature (T_{ref}), $E_{\mathrm{o}}(\mathrm{Ref}_A)$ is the activation energy of A close to T_{ref}, and δ_A describes the change of E_{o} with increasing incubation temperature (T). Similar to respiration parameters, $E_{\mathrm{o}}(\mathrm{Ref}_A)$ and δ_A-values were strongly correlated. Symmetry of A/T curves, i.e., constancy of dE_{o}/dT between 20–45 °C incubation temperatures, suggests close coordination of component processes underlying A. This symmetry remained at high growth temperature, despite large reductions in biochemical capacity for P_{i} regeneration relative to carboxylation capacity (i.e., increased abundance of RubisCO activase). Acclimation to higher temperature caused pronounced reductions in physiological capacity of respiration (R_{Cap}) (type II acclimation, determined via gas exchange measurements). Reductions in R_{Cap} were not a result of limitations in substrate availability (i.e., pyruvate), but were related to lower abundances of mitochondrial enzymes in well-watered plants (i.e., pyruvate dehydrogenase and cytochrome oxidase). Water shortage led to sucrose accumulation, with modest reductions in mitochondrial enzyme pools. R_{Cap} remained low when growth temperature was increased.

Communicated by U. Luettge.

✉ Jörg Kruse
joerg.kruse@ctp.uni-freiburg.de

[1] Chair of Tree Physiology, Institute of Forest Sciences, Georges-Köhler-Allee 53/54, 79110 Freiburg, Germany

[2] Faculty of Agriculture and Environment, The University of Sydney, Sydney, NSW 2006, Australia

[3] College of Sciences, King Saud University, P.O. Box 2455, Riyadh 11451, Saudi Arabia

[4] Department of Plant Systems Biology, University of Hohenheim, 70593 Stuttgart, Germany

Introduction

Plants must cope with large temperature fluctuations on daily, seasonal, and inter-annual time scales. Temperature exerts strong control of biochemical reactions, via the kinetic energy of reactants and the frequency of collisions between substrate molecules and enzymes. Plant respiration, for instance, typically increases exponentially with incubation temperatures (Lambers et al. 1998). Accordingly, instantaneous temperature responses of respiration have long been modeled based on Arrhenius kinetics (Lloyd and Taylor 1994; Xu and Griffin 2006; Clarke 2006; Kruse et al. 2011).

In the longer term (days to weeks), adjustments of leaf respiration (R; μmol m^{-2} s^{-1}) to altered growth temperature must be coordinated with changes of net photosynthesis (A; μmol m^{-2} s^{-1}). Without such coordination, long-lasting perturbations of the balance between net photosynthetic carbon gain and respiratory carbon loss, i.e., the A/R ratio, could seriously impair plant development (i.e., Bunce 2007; Smith and Stitt 2007; Pyl et al. 2012). Full acclimation has been defined as the capability of plants to maintain homeostatic rates of respiration irrespective of growth temperature variation (Kurimoto et al. 2004). Although complete homeostasis is rare (Slot and Kitajima 2015), acclimation helps mediate the balance between supply and demand for carbohydrates under changing environmental conditions (Dewar et al. 1999; Cannell and Thornley 2000; Gifford 2003; Kruse and Adams 2008a, c; Kruse et al. 2013; Amthor 2010; Thornley 2011). For example, water shortages can mitigate temperature acclimation of respiration (Flexas et al. 2006; Maseyk et al. 2008; Rodriguez-Calcerrada et al. 2009; Atkin and Macherel 2009; Chi et al. 2013). Interactive effects between contrasting growth temperature and water availability on respiratory gas exchange, and their relation to underlying biochemical acclimation, have seldom been characterized (Rennenberg et al. 2006)—but are important to understand the large variability in extent of temperature acclimation among species and across environmental conditions (Atkin et al. 2005a, b; Slot and Kitajima 2015).

A large body of evidence supports acclimation of respiration to growth temperatures (e.g., Atkin et al. 2005a, b; Bruhn et al. 2007; Slot and Kitajima 2015). Changes in the slope of the relationship between incubation temperatures and CO_2 evolution are termed 'Type I' acclimation. Changes in basal respiration rates measured at a given low incubation temperature (R_{ref}) are termed 'Type II' acclimation (Atkin et al. 2005a, b). Our current mechanistic understanding about this flexibility of instantaneous temperature responses of leaf dark respiration was previously reviewed by Atkin et al. (2005a, b) and Kruse et al. (2011).

Similar to respiration, acclimation of net photosynthesis can be characterized via measurement of instantaneous temperature responses (Way and Yamori 2014). Instantaneous responses of net assimilation rate (A_T) are generally approximated by a bell-shaped curve within the range of 15–35 °C (Berry and Björkman 1980; Battaglia et al. 1996; Gunderson et al. 2010):

$$A_{(T)} = A_{opt} - b(T - T_{opt})^2 \qquad (1)$$

where T_{opt} is the optimum temperature of carbon fixation (°C), A_{opt} is the 'peak' photosynthesis rate at this optimum temperature (μmol m^{-2} s^{-1}), and the parameter b describes the width of the parabola (dimensionless).

Steady-state rates of A start to decline at temperatures well below those that stimulate peak rates of dark respiration, i.e., at temperatures generally <30 °C (depending on experienced growth temperatures; Gunderson et al. 2010). Instantaneous temperature responses of steady-state photosynthesis have traditionally been interpreted in terms of shifts between rate-limiting processes, as incubation temperature increases (Sage and Kubien 2007; Lin et al. 2012; Yamori et al. 2014). At current atmospheric [CO_2], net CO_2 assimilation of C_3-plants tends to be limited by P_i regeneration at leaf-temperatures <20 °C, by rates of carboxylation via Rubisco between 20 °C up to the thermal optimum (and maybe beyond), and by ribulose-bisphosphate (RuBP) regeneration above the thermal optimum (Sage and Kubien 2007). Leaf temperatures >43–45 °C generally cause irreversible damage to the photosynthetic machinery and rapid decline of A (Seemann et al. 1984), where the upper temperature limits to stable, albeit low, CO_2 assimilation again depends on growth temperature regimes experienced by plants (Hüve et al. 2011).

There is ongoing debate, if the *reversible* decline of A between T_{opt} and the upper temperature limit to stable photosynthetic performance is caused by limitations in maximum velocity of RuBP carboxylation (V_{cmax}), or maximum rate of RuBP regeneration (J_{max}) (Dreyer et al. 2001; Kattge and Knorr 2007; Sage and Kubien 2007; Bernacchi et al. 2013; Yamori et al. 2014). Analysis of temperature dependencies of A/c_i-response curves can theoretically help distinguish, where A becomes limited by J_{max} (Medlyn et al. 2002; Hikosaka et al. 2006; Warren 2008), but the data are often inconclusive (Sage and Kubien 2007; Yamori et al. 2014).

Equation 1 does not readily facilitate identification of physiological limitations to steady-state photosynthesis—including constraints imposed on A by stomatal resistance (Kirschbaum and Farquhar 1984; Lin et al. 2012), and mesophyll resistance to CO_2 transfer (von Caemmerer and Evans 2015). Nonetheless, Eq. 1 does provide a phenomenological description of photosynthetic acclimation. For example, T_{opt} varies with growth temperature for many species (Slayter 1977; Berry and Björkman 1980; Yamasaki et al. 2002; Gunderson et al. 2010), and plasticity in T_{opt} differs widely among species (Battaglia et al. 1996; Warren 2008; Dillaway and Kruger 2010).

Arrhenius models offer potentially straightforward means of identifying 'transition temperature(s)' across a range of incubation temperatures. Any switch between rate-limiting processes in response to increasing incubation temperature should be revealed by temperature-dependent changes of overall activation energy of net photosynthesis (E_{oA}), owing to respective temperature sensitivities of rate-limiting processes. For example, the temperature

sensitivity of sucrose synthesis, which significantly contributes to P_i regeneration capacity, is comparatively large (Leegood and Edwards 1996; Q_{10} of spinach sucrose phosphate synthase (SPS) activity = 2.4, Stitt and Grosse 1988). Arrhenius models of A/T curves coupled with biochemical analyses provide a mechanistic understanding of acclimation processes. For example, cold-grown leaves are richer in SPS-protein than warm-grown leaves (Guy et al. 1992; Hurry et al. 1995; Strand et al. 1999), which helps overcome limitation of A through insufficient P_i regeneration capacity at low growth and incubation temperatures. Cold-grown plants may also exhibit greater amounts of Rubisco (contributing to V_{cmax}), or sedoheptulose-1,7-bisphoshate (contributing to J_{max}; Weih and Karlsson 2001; Stitt and Hurry 2002; Yamori et al. 2005). How enzyme abundances change *in relation* to one another is clearly critical to drawing conclusions about which potential limitation is most sensitive to growth temperature (Sage and Kubien 2007). Unbalanced changes in V_{cmax}, J_{max}, or P_i regeneration should become apparent in the apparent temperature sensitivity of CO_2 assimilation.

We sought to develop a general understanding of acclimation to growth temperature of CO_2-assimilation. We thus extended to photosynthesis, our application of Arrhenius models that can robustly describe instantaneous temperature responses of dark respiration (Kruse et al. 2012; Noguchi et al. 2015). Specifically, our aims were to: (I) identify transition temperatures in A/T curves indicating switches between rate-limiting processes, and how these are affected by elevated growth temperature; (II) determine enzyme abundances involved in RuBP regeneration, carboxylation, and triosephosphate utilization; (III) determine abundances of mitochondrial enzymes and substrate availability used in respiration; and (IV) test how temperature acclimation of photosynthesis and respiration responds to changes of resource availability (water). We used Date palm (*Phoenix dactylifera*) as a test species. Date palm is adapted to hot and semiarid environments (Tengberg 2003).

Materials and methods

Plant material and growth conditions

Two-year old seedlings of Date palm (*P. dactylifera*) were purchased from a commercial supplier ('Der Palmenmann', Bottrop, Germany). Two months before the start of experiments, plants were repotted (2.5-L pots). Pots were filled with a peat–sand–perlite mixture [20:30:50 (vol%)] to which 10 g of NPK fertilizer was added. Plants were grown under greenhouse conditions (15–25 °C, 60–70% rH) and irrigated every second day towards the end of the light period (c. 150–200 ml per pot). After 2 months, plants were transferred to two climate-controlled chambers (Heraeus, Vötsch, Germany). One chamber was set at 20 °C during the light period and 15 °C during the dark period (16 h/8 h; 70 ± 3% relative humidity at day and night), while in the second chamber, plants were exposed to elevated growth temperature during the light period (35 °C at day/15 °C at night; 60 ± 8% relative humidity at day and 70 ± 3% at night). Incident light was the same for both chambers, reaching 200 µmol photons m^{-2} s^{-1} at the leaf level, and plants were arranged to prevent self-shading.

In a first set of experiments, plants continued to be irrigated every second day, including the night before gas exchange measurements ('well-watered' conditions). Plants were given 2 weeks' time to adjust to different temperature regimes between chambers. Experimental setup ensured that plants were exposed for the same time to different growth temperatures. After 2 weeks, instantaneous temperature responses of dark respiration and photosynthesis were determined (2 plants per day and chamber) and the following day plants were harvested—always exactly 6 h after start of the light period. Plant material was frozen in liquid N_2 and stored at −80 °C until further analysis. Measurements lasted 4 consecutive days, so that eight R/T curves and eight A/T curves were available for each growth temperature.

The above experiment was replicated 5 weeks later (in June 2013) with a modification: after 2 weeks of adjustment to different growth temperature, irrigation of 35 °C grown plants was stopped for 4–5 days and that of 20 °C grown plants was stopped for 7–8 days prior to gas exchange measurements. Because of technical limitations (lower relative humidity in the 35 °C-chamber), the duration of water deprivation was 3 days longer for 20 °C grown plants. In an independent experiment conducted 3 months later (September 2013), we quantified the temperature response of V_{cmax} for well-watered plants grown at 20 and 35 °C (6–7 replicates each).

Gas exchange measurements and treatment of temperature responses

Temperature responses of dark respiration were determined via a portable gas exchange measuring system (GFS 3000, Walz, Effeltrich, Germany). Palm leaves were placed into the 8 cm^2 (completely darkened) cuvette of the system that was flushed with air at a defined flow rate of 700 µmol s^{-1}. R/T responses were determined in six 5 °C steps at ambient CO_2 (400 ppm), ranging from 20 to 45 °C. After each temperature change, plants were allowed to equilibrate until steady-state conditions were attained. Subsequently, gas exchange was recorded and averaged over a period of 5 min (Fig. 1a).
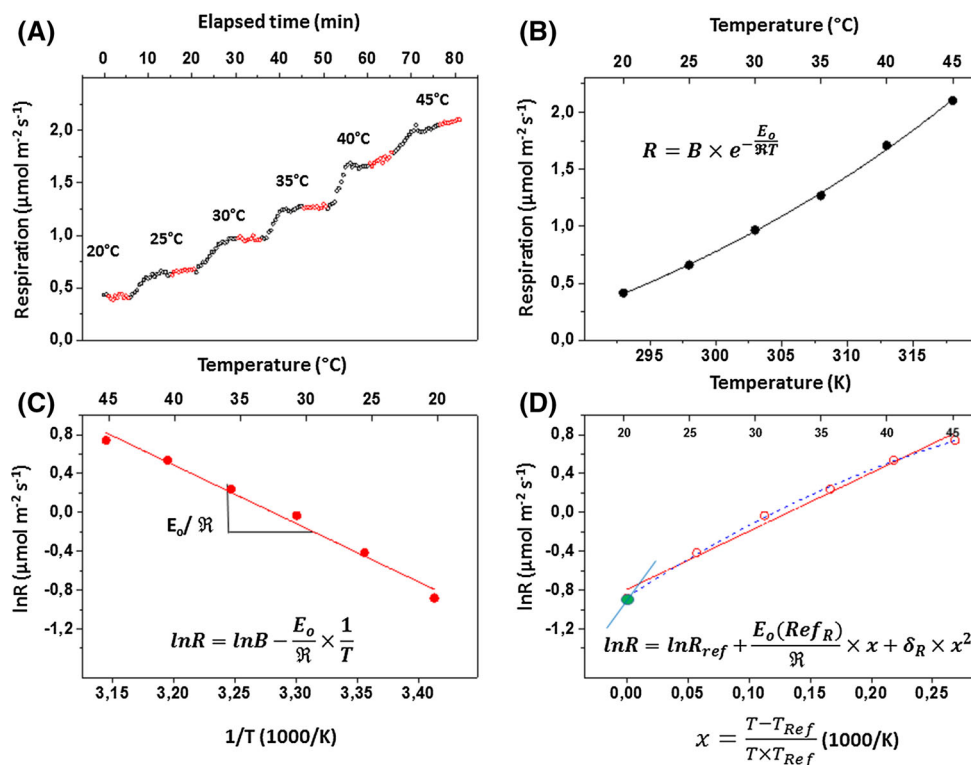
Fig. 1 Protocol of gas exchange measurements. **a** Response of steady-state respiration in the dark to stepwise increase of cuvette temperatures. The same protocol was applied to photosynthesis measurements in the light (PAR: 1200 µmol m^{-2} s^{-1}). **b** Temperature response of respiration. The temperature response of respiration can be *approximated* by the Arrhenius function. **c** Linearized expression of the respiratory temperature response shown in **b**. The *average* activation energy of the process can be calculated form the slope of

ln$R$ plotted against $1/T$. **d** Modification of the Arrhenius equation to account for changes in E_{oR} with increasing incubation temperature. $E_o(Ref_R)$ denotes the slope of the curve at the reference temperature. The parameter δ_R describes how this slope (i.e., E_{oR}) changes with increasing incubation temperature. The R^2 of this exemplary fit was 0.99. Average R^2 of Arrhenius-type fits of all R/T responses was 0.976, and that of A/T responses was 0.95 (see Fig. 2e)

The temperature response of respiration ($R_{(T)}$) can be fully described by a three-parameter exponential equation (Kruse et al. 2011; Noguchi et al. 2015), derived from the original Arrhenius equation. The original Arrhenius equation is given by (Atkins and de Paula 2006):

$$k = Be^{-\frac{E_a}{\Re T}} \quad (2)$$

where k is the rate constant of a reaction, E_a is the activation barrier to the reaction, $\Re$ is the universal gas constant (8.314 J mol^{-1} K^{-1}), T is the incubation temperature (K), and the pre-exponential constant B is a frequency-factor. Instantaneous temperature responses of respiration *approximate* Arrhenius kinetics (Fig. 1b), where the *average* 'overall' activation energy E_o (kJ mol^{-1}) can be calculated from the slope of ln$R$ plotted against $1/T$ (Fig. 1c). The Arrhenius equation is valid for single chemical reactions, but can be applied to a *network* of enzymatic processes involved in dark respiration (R_T). In representing respiration, Lloyd and Taylor (1994) normalized Eq. 1 to a fixed reference temperature:

$$R_T = R_{ref} \times e^{\frac{E_o}{\Re} \times \left[\frac{1}{T_{ref}} - \frac{1}{T}\right]} \quad (3)$$

where R_{ref} are rates of dark respiration (µmol m^{-2} s^{-1}) at the reference temperature (T_{ref}; 293 K in this study). Kruse and Adams (2008b) further modified Eq. 3 to account for the 'dynamic response' of respiration (Atkin and Tjoelker 2003) to incubation temperature:

$$R_T = R_{ref} \times e^{\left[\frac{E_o(Ref_R)}{\Re} \times \left(\frac{T-T_{ref}}{T \times T_{ref}}\right) + \delta_R \times \left(\frac{T-T_{ref}}{T \times T_{ref}}\right)^2\right]} \quad (4)$$

where $E_o(Ref_R)$ is the 'overall' activation energy of respiration (infinitesimally) close to the reference temperature (kJ mol^{-1}), and δ_R (kK^2) is the 'dynamic response' of respiration to incubation temperature. More precisely, δ_R describes the change in slope of E_{oR} with changing incubation temperature (Noguchi et al. 2015; Fig. 1d). The temperature sensitivity of activation energy often declines with increasing incubation temperature (i.e., $\delta_R < 0$) (Tjoelker et al. 2001; Kruse et al. 2012; Noguchi et al.

2015), but peak rates of respiration are generally recorded at temperatures >45 °C (O'Sullivan et al. 2013). In biological terms, variation in δ_R reflects variation in flux modes of respiratory metabolism (Kruse et al. 2008, 2011). The three parameters of this equation can be determined from the linearized expression of Eq. 4, as described in Fig. 1d.

A fourth parameter can be obtained from the linearized expression of those temperature responses, defined as the 'respiratory capacity' (R_{Cap}). Respiratory capacity is often equated with R_{ref} (Smith and Dukes 2013), but, as shown recently, R_{ref} is not fully independent of the relationship between incubation temperature and CO_2-evolution (Kruse et al. 2008; Noguchi et al. 2015)—making it difficult to distinguish between 'Type I' and 'Type II' acclimation. Instead of being characterized by point measurements, R_{Cap} is better defined as an integrative parameter spanning a range of incubation temperatures (Kruse et al. 2011, 2012). Substituting the temperature term $\frac{T-T_{ref}}{T \times T_{ref}}$ by x, R_{Cap} was calculated as the integral from 0 to u, where the upper boundary u is given by the highest incubation temperature (i.e., 318 K, so that $u = 0.268$ in this study):

$$R_{Cap} = \int_0^u F_{(x)} dx$$
$$= \ln R_{ref} \times x + \frac{1}{2}\frac{E_o(Ref_R)}{\Re} \times x^2 + \frac{1}{3}\delta_R \times x^3 - C \big|_0^u$$
(5)

where $x = \frac{T-T_{ref}}{T \times T_{ref}}(1000/K)$, $\ln R_{ref}$ is the (logarithmic) respiration rate at the reference temperature given in nmol m^{-2} s^{-1} (area basis), and C is a scaling constant related to the single lowest $\ln R_{ref}$ value that was observed [$C = (\ln R_{ref})_l \times u$]. This approach deviates from the one described by Kruse et al. (2011), who defined R_{Cap} on the basis of plant mass with R_{ref} given in nmol g^{-1} s^{-1} (mass basis), so that $\ln R_{ref} > 0$. The introduction of the scaling constant C into Eq. 5 emphasizes that R_{Cap} is expressed in relative units (dimensionless; compare Table 1). In biological terms, the physiological capacity of leaf dark respiration (R_{Cap}) partly depends on mitochondrial enzyme abundances or, more generally, on leaf-nitrogen content (Miroslavov and Kravkina 1991; Armstrong et al. 2006; Atkin et al. 2015); but R_{Cap} may also vary with substrate supply to mitochondria (i.e., pyruvate delivered by glycolysis; Givan 1999).

Steady-state rates of net CO_2-assimilation at each of the six incubation temperatures were recorded under ambient CO_2 (400 ppm), saturating light intensity (PPFD: 1200 µmol m^{-2} s^{-1}), and 13,000 ppm H_2O (incoming air). Cuvette temperature was measured by Pt100 sensors and regulated via Peltier elements (accuracy ± 0.1 °C after 3 min equilibration). Leaf temperature was determined via a thermocouple that measures a differential temperature signal (accuracy ± 0.2 °C), i.e., the difference between the temperature at its tip touching the lower leaf surface and a reference within the cuvette (GFS 3000, Walz, Effeltrich, Germany). Vapor pressure deficit in the cuvette increased from 15 Pa/kPa at 20 °C to 95 Pa/kPa at 45 °C. A/T curves were fitted to an equivalent, 'linearized' expression of Eq. 4:

$$\ln A_T = \ln A_{ref} + \frac{E_o(Ref_A)}{\Re} \times \left(\frac{T-T_{ref}}{T \times T_{ref}}\right) + \delta_A$$
$$\times \left(\frac{T-T_{ref}}{T \times T_{ref}}\right)^2,$$
(6)

where $\ln A_{ref}$ are (logarithmic) rates of net CO_2-assimilation at the reference temperature (µmol m^{-2} s^{-1}), $E_o(Ref_A)$ (kJ mol^{-1}) is the activation energy of photosynthesis (infinitesimally) close to the reference temperature, and δ_A (kK^2) describes how the activation energy of A changes with incubation temperature. Setting $\frac{T-T_{ref}}{T \times T_{ref}} = x$, the optimum temperature of A (T_{opt}), where peak rates of photosynthesis were reached, was determined from the first derivative of Eq. 6 (i.e., $d\ln A/dx = 0$):

$$x_{opt} = -\frac{E_o(Ref_A)}{2\Re \times \delta_A},$$
(7)

where $x_{opt} = \frac{T_{opt}-T_{ref}}{T_{opt} \times T_{ref}}(1000/K)$ and $\delta_A < 0$. Peak rates of photosynthesis (A_{opt}) and photosynthesis at growth temperature (A_{growth}) were determined by insertion of x_{opt} and x_{growth} into Eq. 6. A_{growth} may significantly depart from A_{opt} (Way and Yamori 2014).

In an independent experiment, the temperature response of V_{cmax} was determined via A/C_i response curves conducted at 20, 26, 32, and 38 °C with the same leaf at saturating light (1200 µmol m^{-2} s^{-1}) (Sharkey et al. 2007). Temperature dependency of V_{cmax} of individual leaves was determined consecutively, starting with 20 °C incubation temperature. For each incubation temperature, measurements started at 400 ppm CO_2. Ambient CO_2 was reduced stepwise to 50 ppm CO_2 and measurements at each CO_2-concentration took about 15 min (including equilibration, recording of zero point, and recording of 5 min average of net assimilation rate). Subsequently, the CO_2 range above ambient was covered. When A is CO_2 limited, the response of A to [CO_2] can be described as follows (Farquhar et al. 1980; von Caemmerer 2013):

$$A_c = V_{cmax}\left[\frac{C_i - \Gamma^*}{C_i + K_c(1 + O/K_O)}\right] - R_l,$$
(8)

where V_{cmax} is the maximum velocity of Rubisco for carboxylation, C_i is the substomatal partial pressure of CO_2, K_c is the Michaelis constant of Rubisco for carbon dioxide, O is the partial pressure of oxygen, and K_o is the Michaelis

Trees (2017) 31:623–644

Table 1 List of symbols and abbreviations used in this study

Photosynthesis			
A_{ref}	$\mu\mathrm{mol\ m^{-2}\ s^{-1}}$	Net photosynthesis at the reference temperature	
A_{growth}	$\mu\mathrm{mol\ m^{-2}\ s^{-1}}$	Net photosynthesis at growth temperature	
A_{opt}	$\mu\mathrm{mol\ m^{-2}\ s^{-1}}$	Peak rates of net photosynthesis at optimum temperature (=physiological capacity of A)	
T_{ref}	K	Low reference temperature (293 K in this study)	
T_{opt}	K or °C	Optimum temperature of A	
E_{oA}	$\mathrm{kJ\ mol^{-1}}$	Activation energy of A at some (unspecified) incubation temperature	
$E_{\mathrm{o}}(\mathrm{Ref}_A)$	$\mathrm{kJ\ mol^{-1}}$	Activation energy of A infinitesimally close to (or 'at') the reference temperature	
δ_A	$\mathrm{kK^2}$	Dynamic response of E_{oA} to changes in incubation temperature	
V_{cmax}	$\mu\mathrm{mol\ m^{-2}\ s^{-1}}$	Maximum velocity of RubP carboxylation	
Dark respiration			
R_{ref}	$\mu\mathrm{mol\ m^{-2}\ s^{-1}}$	Respiration at the reference temperature	
R_{growth}	$\mu\mathrm{mol\ m^{-2}\ s^{-1}}$	Respiration at growth temperature	
R_{Cap}	Dimensionless	Physiological capacity of dark respiration	
E_{oR}	$\mathrm{kJ\ mol^{-1}}$	Activation energy of R at some (unspecified) incubation temperature	
$E_{\mathrm{o}}\ (\mathrm{Ref}_R)$	$\mathrm{kJ\ mol^{-1}}$	Activation energy of R infinitesimally close to (or 'at') the reference temperature	
$E_{\mathrm{o}}\ (\mathrm{Growth}_R)$	$\mathrm{kJ\ mol^{-1}}$	Activation energy of R at growth temperature	
δ_R	$\mathrm{kK^2}$	Dynamic response of E_{oR} to changes in incubation temperature	

constant of Rubisco for oxygen; Γ^* is the photorespiratory compensation point and R_1 is respiratory CO_2 release other than by photorespiration and is presumed to be primarily mitochondrial respiration ('light respiration'; not determined in this study). Equation 8 lends itself to a linear regression approach to estimating V_{cmax} (Long and Bernacchi 2003). Parameter values of Γ^*, $K_{\mathrm{c,}}$ and K_{o} at different incubation temperatures (20, 26, 32, and 38 °C) were determined according to Bernacchi et al. (2001). Calculations of temperature-dependent V_{cmax} for date palm are estimates, because temperature sensitivity of Γ^*, $K_{\mathrm{c,}}$ and K_{o} is, to date, only available for tobacco and *Arabidopsis thaliana* (Bernacchi et al. 2001; Walker et al. 2013). Calculated V_{cmax} according to Eq. 8 yields 'apparent' values, because temperature effects on mesophyll conductance and C_{c} (i.e., CO_2 partial pressures at the site of carboxylation), were not considered (Warren and Dreyer 2006; Diaz-Espejo 2013; Walker et al. 2013). V_{cmax} was estimated for $C_{\mathrm{i}} <220$ ppm—well within the CO_2 limited range of photosynthesis (Long and Bernacchi 2003). In this study, we did not determine J_{max}, because $[CO_2] >$ ambient led to rapid closure of stomata in *P. dactylifera*. For example, application of 1500 ppm CO_2 was not sufficient to increase C_{i} above 600 ppm CO_2.

Determination of total leaf-nitrogen and extraction of proteins

Area and fresh mass of leaves used for gas exchange measurements were recorded. For total leaf-N analysis, part of the leaf fresh mass was dried at 65 °C, while the other part was frozen in liquid N_2 and stored at -80 °C. For analysis of total leaf-N, aliquots of 1.5–2.0 mg of dried and ground plant material were transferred into tin capsules (IVA Analysentechnik, Meerbusch, Germany). Nitrogen content of samples was determined using an elemental analyzer (Vario EL, Elementar-Analyse Systeme GmbH, Hanau, Germany), and related to leaf area.

Proteins were extracted from 150 mg of ground and frozen plant material, using 50 mM Tris–HCl buffer (pH 8), which contained 1 mM EDTA, 5 mM DTT, 1 mM PMSF, 15% glycerol (v/v), and 0.1% Triton X-100 (v/v). Extracted proteins were washed twice with 80% acetone and subsequently dried for 30 min on ice.

Proteome analysis

Extracted proteins were precipitated using TCA and re-suspended in a mixture 6 M urea 2 M thiourea pH 8 before pre-digestion for 3 h with endoproteinase Lys-C (0.5 µg µL^{-1}; Wako Chemicals, Neuss). After fourfold dilution with 10 mM Tris–HCl (pH 8), samples were digested with 4 µL Sequencing Grade Modified trypsin (0.5 µg µL^{-1}; Promega). Digested peptides were desalted over a C18 STAGE tips (Rappsilber et al. 2003) before mass spectrometric analysis. LC–MS/MS analysis was performed with a total of 5 µg of peptides from each sample, using nanoflow Easy-nLC1000 (Thermo Scientific, Dreieich, Germany) as an HPLC system and a Quadrupole–Orbitrap hybrid mass spectrometer (Q-Exactive Plus, Thermo Scientific, Dreieich Germany) as mass analyzer.
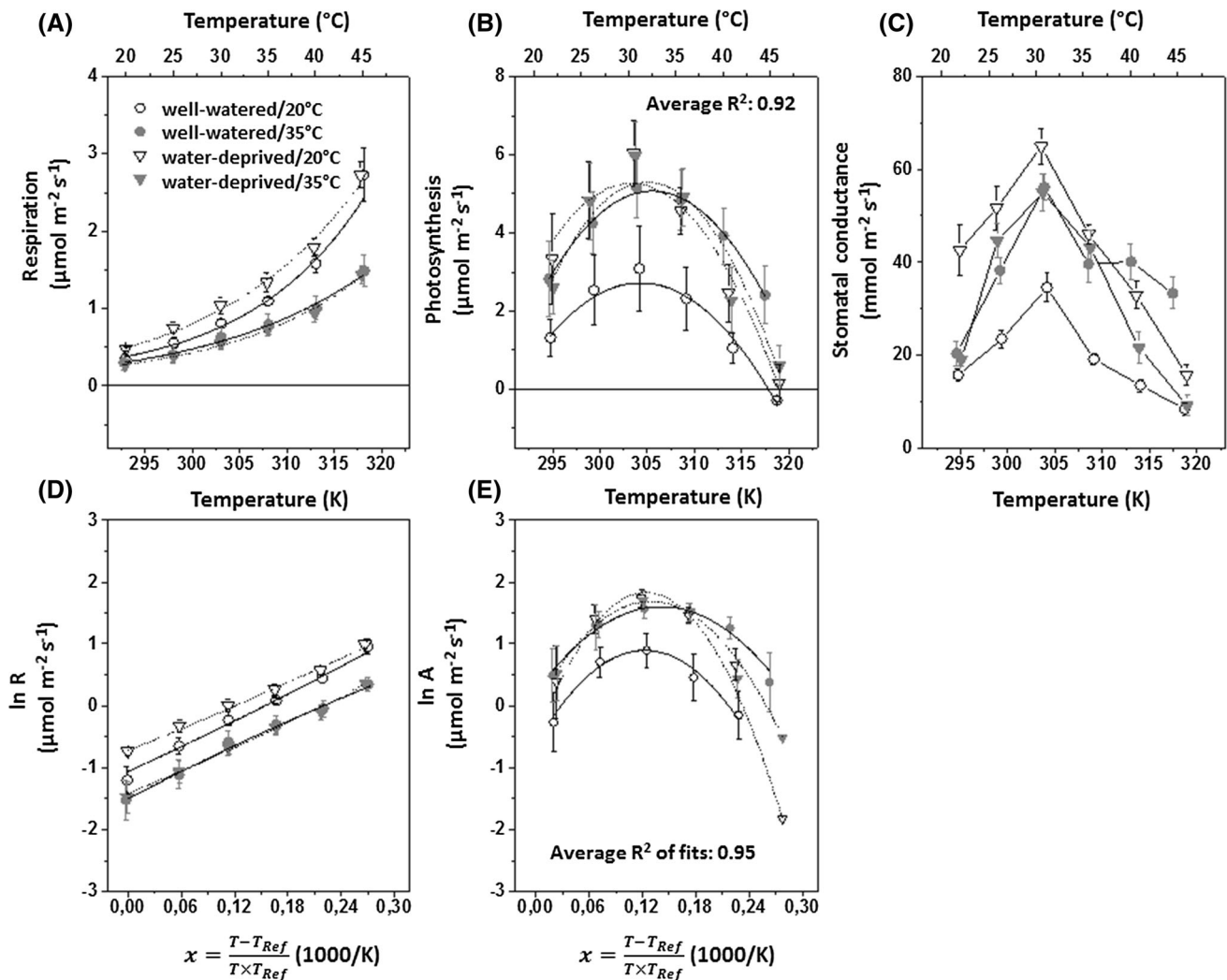
🙋 Springer

Fig. 2 Temperature responses of respiration and photosynthesis. **a** Exponential increase of respiration with incubation temperature, as affected by growth temperature (20 vs. 35 °C) and water availability ('well-watered' vs. 'water-deprived'). **b** Parabolic temperature response of photosynthesis, as affected by growth temperature and water availability. **c** Temperature response of stomatal conductance (g_s). **d** Linearized expression of the respiratory temperature response. Note that on average, E_{oR} was constant (zero temperature sensitivity, i.e., $\delta_R = 0$). **e** 'Linearized' expression of the photosynthetic temperature response. The relation between photosynthesis and incubation temperature is often described by a parabolic function with a distinct optimum (cf. **b**). Photosynthesis data can also be fitted using the three-parameter model that describes the temperature response of respiration. Data shown are averages ± SE of eight independent replicates, each. Treatment effects on parameter values of temperature responses are depicted in Fig. 4 and Table 3

Proteins were identified and ion intensity was quantified using MaxQuant version 1.4.0.1 (Cox and Mann 2008). Spectra were matched against a translation of the date palm transcriptome (PDK30-pep, 28889 entries) using Andromeda (Cox et al. 2011).

Metabolite analysis

Metabolites were analyzed as described by Kreuzwieser et al. (2009). In brief, 50 mg of homogenized and frozen plant material was extracted in 700 µL of 100% methanol, at 70 °C. Samples were derivatized in a solution containing methoxyamine (20 mg mL^{-1} pyridine). After addition of silylating agent MSTFA, samples were subjected to GC–MS analysis. Metabolites were separated via gas chromatography (Agilent Technologies 7890A, Frankfurt, Germany), coupled to a mass spectrometer (Agilent Technologies 5975C MS, Frankfurt, Germany). Data were analyzed with AMDIS software package (http://chemdata.nist.gov/mass-spc/amdis/), and metabolites were identified using the Golm metabolome (Kopka et al. 2005; Schauer et al. 2005).

Fig. 3 Correlation between the activation energy of gas exchange (infinitesimally) close to the low reference temperature (E_o(Ref); T_{ref} = 20 °C) and the change of activation energy with increasing incubation temperature (as described by the δ-parameter). **a** Correlation between E_o(Ref$_A$) and δ_A derived from Arrhenius-type fits of A/T curves. **b** Correlation between E_o(Ref$_R$) and δ_R derived from Arrhenius-type fits of R/T curves (see Fig. 1d). Each data point was derived from individual temperature response curves spanning 20–45 °C (six 5 °C-intervals)
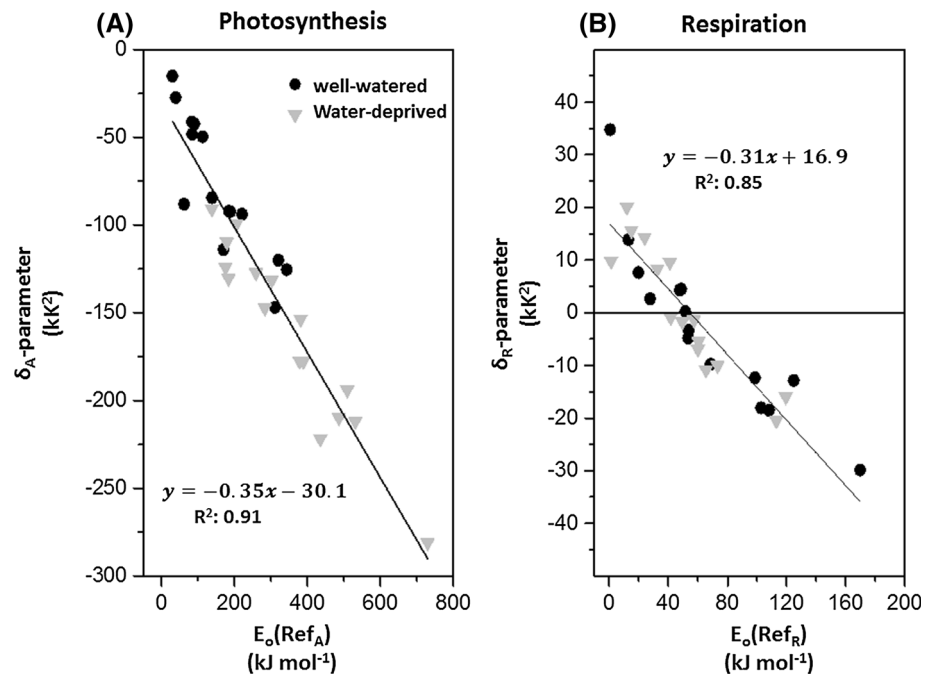
Table 2 Effects of growth temperature and water availability on dry mass: fresh mass ratio (DW/FW) and specific leaf area (SLA)

	Well-watered		Drought		Temp. (T)	Water (W)	$T \times W$
	20 °C	35 °C	20 °C	35 °C			
DW/FW (g g^{-1})	0.395 ± 0.007	0.375 ± 0.008	0.344 ± 0.007	0.366 ± 0.016	n.s.	$p < 0.01$	$p < 0.01$
SLA (cm^2/gDW)	35.4 ± 0.8	37.3 ± 1.0	41.2 ± 0.9	38.1 ± 1.4	n.s.	$p < 0.01$	$p < 0.01$

Data shown are averages ± SE of eight replicates (plants). Data were subjected to two-way ANOVA to assess the significance of water availability (W) and growth temperature (T) for biometric parameters

Statistical analysis

Statistical analysis used eight independent replicates per treatment for gas exchange parameters and metabolites, and five replicates for peptide analysis. Data analysis of peptides followed Zauber and Schulze (2012). For metabolite analysis, peak areas of respective metabolites were related to leaf area (like N-contents and gas exchange). Treatment effects on metabolites were expressed as changes in relative abundance. For this purpose, individual peak areas (P_i) were related to the average of 32 samples (P_a), so that relative deviation from the average (P_r) was calculated as P_i/P_a. Data of P_r, peptide abundances and gas exchange parameters were submitted to two-way ANOVA, to evaluate the significance of growth temperature and water availability for these variables (STATISTCA, version 10.0, StatSoft, Inc, Tulsa, OK, USA).

Results

Temperature responses of photosynthesis and respiration

Temperature responses of respiration and photosynthesis differed significantly (Fig. 2a, b). Rates of photosynthesis were greatest at 'moderate' incubation temperatures of 30 ± 3 °C, and temperature responses of A were not exponential. Respiration, on the other hand, increased exponentially with applied temperature (Fig. 2a). Overall, temperature responses of respiration followed linear Arrhenius kinetics (Fig. 2d), and δ_R values were close to zero. Even so, the three-parameter model used to fit respiration data, also accurately describes the temperature response of photosynthesis (Fig. 2e). R^2 values of Arrhenius-type fits of A/T curves averaged 0.95 (Fig. 2e) and were somewhat more than average R^2 of parabolic fits
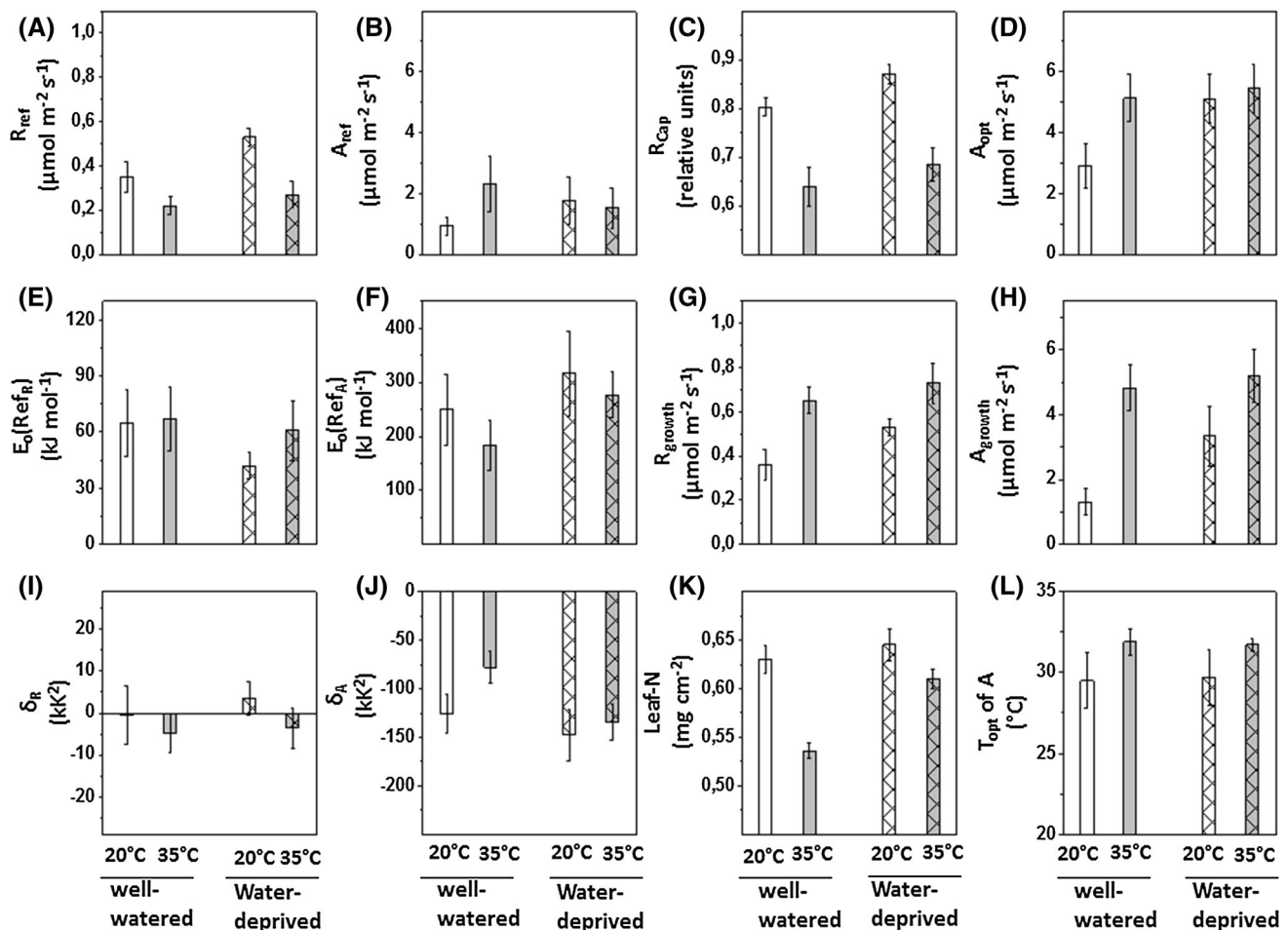
Fig. 4 Treatment effects on parameter values of the temperature response of respiration and photosynthesis. **a** Rates of respiration at the reference temperature (20 °C), as affected by growth temperature and water availability. **b** Rates of photosynthesis at the reference temperature. **c** Respiratory capacity (R_{Cap}) as affected by drought and growth temperature. **d** Peak rates of photosynthesis at the optimum temperature. **e** Activation energy of respiration at the reference temperature. **f** Activation energy of photosynthesis at the reference temperature. **g** Rates of respiration at the respective growth temperature (20 or 35 °C). **h** Rates of photosynthesis at the respective growth temperature (20 or 35 °C). **i** Sensitivity of E_{oR} to incubation temperature (δ_R-parameter). **j** Sensitivity of E_{oA} to incubation temperature (δ_A-parameter). **k** Leaf-nitrogen contents. **l** Optimum temperature at which peak rates of photosynthesis were achieved. Each *column* shows the average ± SE of eight independent replicates. Data were subjected to two-way ANOVA to assess the significance of growth temperature and water availability for gas exchange parameters (see Table 3)

(Fig. 2b) (for further exploration see companion study, Kruse et al. 2016).

Strikingly, the two parameters E_o(Ref) and δ were strongly correlated, for both respiration and photosynthesis (Fig. 3a, b), suggesting that temperature responses of photosynthesis and respiration share common features, albeit with clear differences for E_o(Ref) and δ. For respiration, δ_R was frequently positive, and $\delta_R = 0$ at E_o(Ref$_R$) = 54.5 kJ mol^{-1} (Fig. 3b). For photosynthesis, δ_A was always negative (Fig. 3a). Second, water deprivation significantly reduced δ_A (compared with well-watered plants), but did not affect δ_R. As a result, the parabolic relation between photosynthesis and incubation temperature was more narrow in water-deprived than in well-watered plants (Fig. 2b). The temperature response of stomatal conductance (g_s) and the

effect of water deprivation on this response were similar to that of CO_2-assimilation. There was a sharper *increase* in g_s at low incubation temperatures followed by a sharper *decrease* in g_s at high temperatures when compared with well-watered plants (Fig. 2c).

Characterization of respiratory and photosynthetic acclimation, based on parameters derived from instantaneous temperature responses

Water deprivation decreased DW/FW of date palm leaves and depended on growth temperature. DW/FW of well-watered plants was less for plants grown at 35 °C than 20 °C. This pattern was reversed in water-deprived plants (Table 2).

Table 3 Results of ANOVA, testing for the effects growth temperature (T), and water availability (W) (and their interaction $T \times W$) on parameters of R/T and A/T curves, enzyme abundances, and leaf metabolite levels

	T	W	$T \times W$		T	W	$T \times W$
Respiration parameters (Fig. 4)				Photosynthesis parameters (Fig. 4)			
R_{ref}	<0.05	0.08	n.s.	A_{ref}	n.s.	n.s.	n.s.
$E_o(Ref_R)$	n.s.	n.s.	n.s.	$E_o(Ref_A)$	0.14	0.08	n.s.
δ_R	n.s.	n.s.	n.s.	δ_A	0.09	<0.05	n.s.
R_{Cap}	<0.001	0.09	n.s.	A_{opt}	0.06	0.07	0.06
R_{growth}	<0.001	<0.01	n.s.	A_{growth}	<0.001	<0.05	<0.05
Leaf-N	<0.001	n.s.	<0.05	T_{opt}	0.08	n.s.	n.s.
Glycolytic enzymes (Fig. 9)				Enzymes involved in RuBPcarboxylation, regeneration, and P_i regeneration (Fig. 5)			
Phoshoglucomutase	n.s	n.s	<0.05	Ferredoxin-reductase	n.s.	n.s.	n.s.
Glu-6P-DH	n.s	n.s	n.s	RubisCO	n.s.	n.s.	n.s.
Glu-6P-Iso.	0.08	n.s	n.s	RubisCO-activase	<0.001	n.s.	n.s.
PFK	n.s	n.s	<0.05	NADP-glycerald-3P-DH	n.s.	n.s.	n.s.
PP$_i$-PFK	n.s	n.s	<0.01	Sedohept.-1,7-P$_2$-ase	n.s.	n.s.	n.s.
Fru-P$_2$-aldolase	<0.05	n.s	<0.05	Transaldolase	n.s.	n.s.	n.s.
Triose-P-isomerase	n.s	n.s	n.s	Transketolase	n.s.	n.s.	n.s.
NAD-glycerald.-3P-DH	n.s	n.s	n.s	Phosphoribulokinase	n.s.	n.s.	<0.05
Phoshoglycerate-kinase	n.s	n.s	n.s	ADP-glucose-phosphorylase	n.s.	n.s.	<0.01
Enolase	<0.05	<0.05	n.s	UDP-glucose-phosphorylase	n.s.	n.s.	<0.05
Pyruvate kinase	n.s	n.s	<0.05	Sucrose-P-synthase	<0.01	n.s.	n.s.
PEP-carboxylase	n.s	n.s	<0.05	Fructose-6P-2 kinase	<0.001	n.s.	n.s.
Mitochondrial enzymes (Fig. 8)				Leaf-metabolites (Fig. 10)			
Pyruvate-DH	<0.01	n.s.	0.08	Glucose	n.s.	<0.001	n.s.
Citrate synth.	n.s.	n.s.	<0.05	Fructose	n.s.	<0.01	n.s.
NADP-isocit.-DH	<0.05	n.s.	<0.01	Sucrose	n.s.	<0.001	<0.01
NAD-isocit.-DH	n.s.	n.s.	<0.01	Oxalate	<0.01	<0.001	n.s.
Succinate-DH	n.s.	<0.05	n.s.	Malate	0.07	<0.001	n.s.
Fumarase	n.s.	n.s.	n.s.	Pyruvate	n.s.	0.08	<0.05
Malate-DH	<0.05	n.s.	<0.05	Citrate	<0.05	n.s.	n.s.
NADH-ubiqu.-oxidoreduct.	n.s.	n.s.	<0.05	Succinate	<0.01	n.s.	n.s.
Cyt-c-oxidase	n.s.	n.s.	<0.01				

Data shown are p values

N.s. not significant (i.e., $p > 0.1$)

After 2 weeks of growth at 35 °C, respiratory capacity (R_{Cap}) was reduced by 20% compared with 20 °C grown plants for both well-watered and 'dry' conditions (Fig. 4c; Table 3). After a few days of water shortage, R_{Cap} was enhanced by 5–10% compared with well-watered conditions (significant at $p < 0.1$; Fig. 4c; Table 3). We observed similar treatment effects on R_{ref} (Fig. 4a) and leaf-nitrogen concentrations (Fig. 4k), although at high growth temperature (35 °C), water shortage led to a larger increase in N concentration than in R_{Cap} or R_{ref} (significant interaction between $T \times W$ on leaf-N, Table 3). Even though increased growth temperature reduced R_{Cap}, it concomitantly increased R_{growth} (Fig. 4g). R_{growth} was also enhanced in response to water deprivation. Neither growth temperature nor irrigation treatment had significant effects on $E_o(Ref_R)$ (Fig. 4e) or δ_R (Fig. 4i).

Growth temperature did not significantly affect A_{ref} (Fig. 4b), but slightly decreased $E_o(Ref_A)$ ($p = 0.14$; Fig. 4f) and increased δ_A ($p = 0.09$; Fig. 4j). Water deprivation increased $E_o(Ref_A)$ ($p = 0.08$; Fig. 4f) and decreased δ_A ($p = 0.04$; Fig. 4j) (see Table 3 for the results of ANOVA).

Increased growth temperature had only a minor effect on T_{opt}, ranging from 29.5 ± 1.7 °C in 20 °C grown plants to 31.5 ± 0.6 °C in 35 °C grown plants (Fig. 4l; $p = 0.08$, Table 3). Increased growth temperature increased A_{opt} by c. 60% in well-watered plants, but only marginally increased A_{opt} in water-deprived plants (Fig. 4d). Effects of growth temperature and water deprivation were more pronounced for A_{growth} (Fig. 4h). Both increased growth temperature and water deprivation significantly increased A_{growth} (Table 2). These effects resembled those of R_{growth},
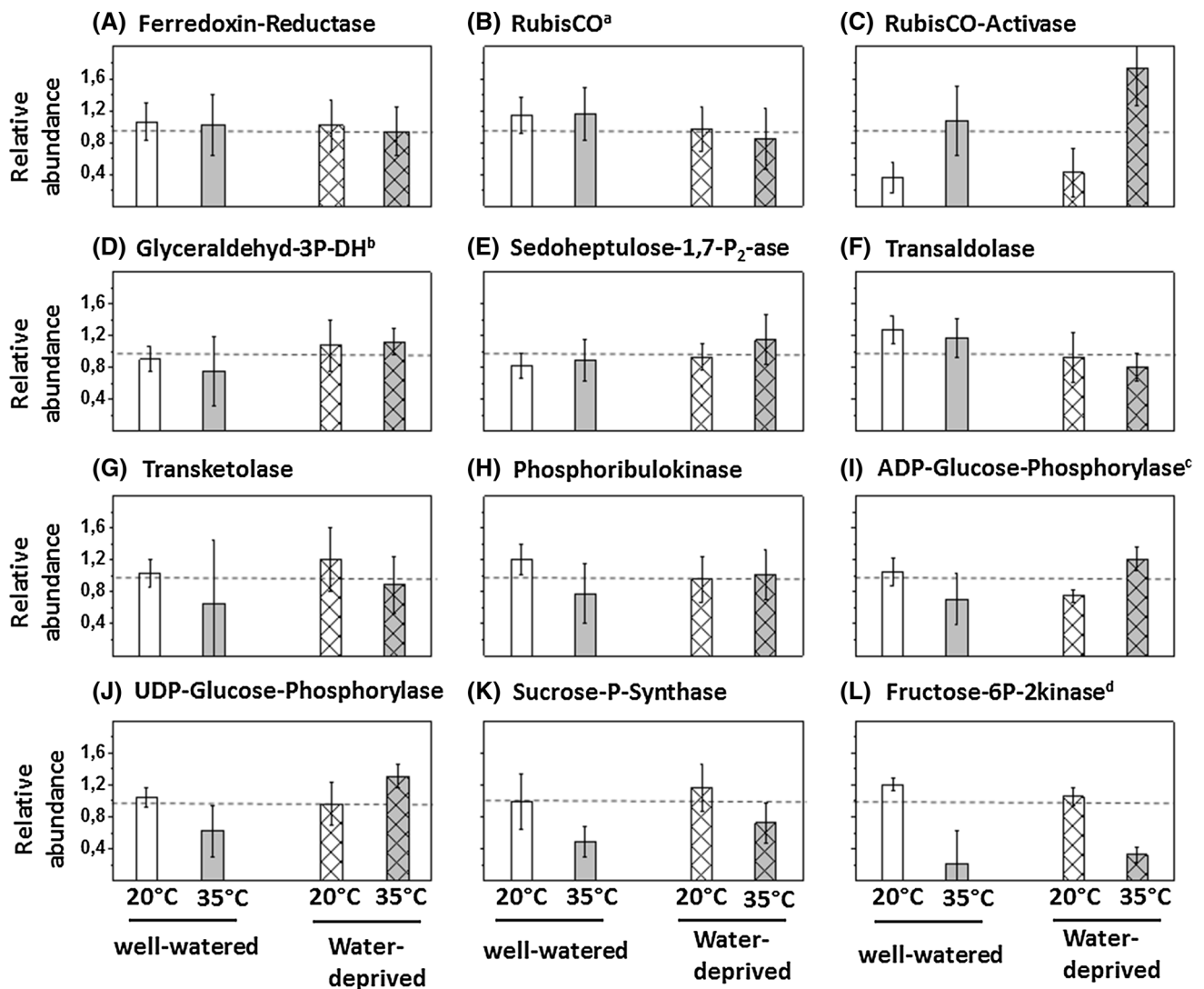
Fig. 5 Treatment effects on abundances of enzymes contributing to V_{cmax}, J_{max}, or P_i regeneration capacity. Enzyme 'abundances' relate to a total of 5 µg of peptides (from each replicate) subjected to mass spectrometric analysis. **a** Ferredoxin-NADP oxidoreductase. **b** Ribulose-1,5-bisphosphate carboxylase/oxygenase ([a]small subunit). **c** RubisCO-activase. **d** Glyceraldehyde-3P-dehydrogenase ([b]NADP-dependent plastidic isoform). **e** Sedoheptulose-1,7-bisphosphatase. **f** Transaldolase. **g** Transketolase. **h** Phosphoribulokinase. **i** ADP- Glucose-pyrophosphorylase ([c]large subunit). **j** UDP-glucose-pyrophosphorylase. **k** Cytosolic sucrose-P-synthase. **l** [d]Fructose-6P-2kinase-fructose-2,6-bisphosphatase (unique cytosolic enzyme with dual catalytic function). Each *column* shows the average ± SE of five independent replicates. Data were subjected to two-way ANOVA to assess the significance of growth temperature and water availability for abundance of individual proteins (see Table 3)

such that the ratio of A_{growth}/R_{growth} remained almost constant (see Supplementary Information; Fig. S1).

Factors controlling acclimation of photosynthesis to heat and drought

Growth temperature and water availability had a little effect on enzymes involved in RuBP regeneration capacity (J_{max}) (Table 3). There were no significant effects on abundances of ferredoxin-NADP oxidoreductase (Fig. 5a), NADP-dependent glyceraldehyde-3P-dehydrogenase (Fig. 5d),

sedoheptulose-1,7-bisphosphatase (Fig. 5e), transaldolase (Fig. 5f), or transketolase (Fig. 5g).

Abundances of Rubisco (contributing to V_{cmax}) were also not affected by growth temperature and water availability (Fig. 5b). On the other hand, abundances of Rubisco activase (Fig. 5c) were strongly increased under 35 °C growth temperature (Table 3).

Abundances of key enzymes for starch synthesis, ADP-glucose pyrophosphorylase (Fig. 5i), and for sucrose synthesis, UDP-glucose pyrophosphorylase (Fig. 5j) were significantly reduced when well-watered plants were

Fig. 6 Temperature dependency of the A/c_i response of data palm seedlings acclimated to 20 and 35 °C. **a** A/c_i response at 20 °C. **b** A/c_i response at 26 °C. **c** A/c_i response at 32 °C. **d** A/c_i response at 38 °C. V_{cmax} was calculated for c_i <220 ppm, i.e., for the linear range of the response curve. Each data point represents the average ± SD of 6–7 independent replicates (leaves)
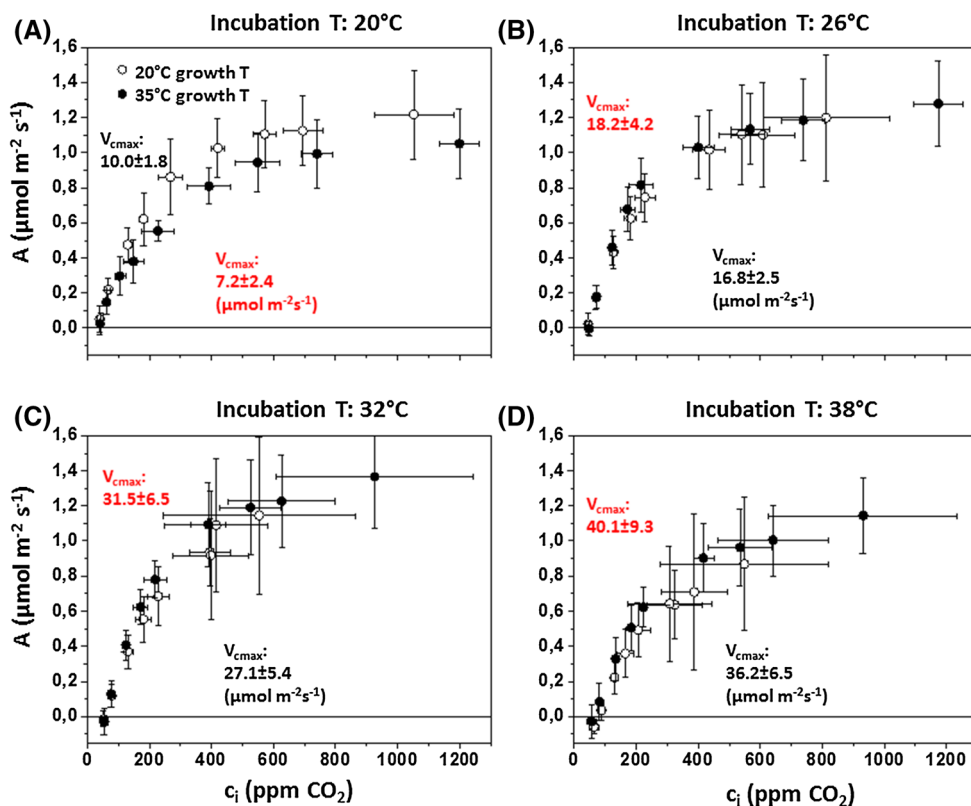

Fig. 7 Sensitivity of stomatal conductance (g_s) to applied CO_2 and growth temperature. **a** Stomatal conductance at 20 °C incubation temperature. **b** Stomatal conductance at 26 °C incubation temperature. **c** Stomatal conductance at 32 °C incubation temperature. **d** Stomatal conductance at 38 °C incubation temperature. Each *column* shows the average ± SE of 6–7 independent replicates
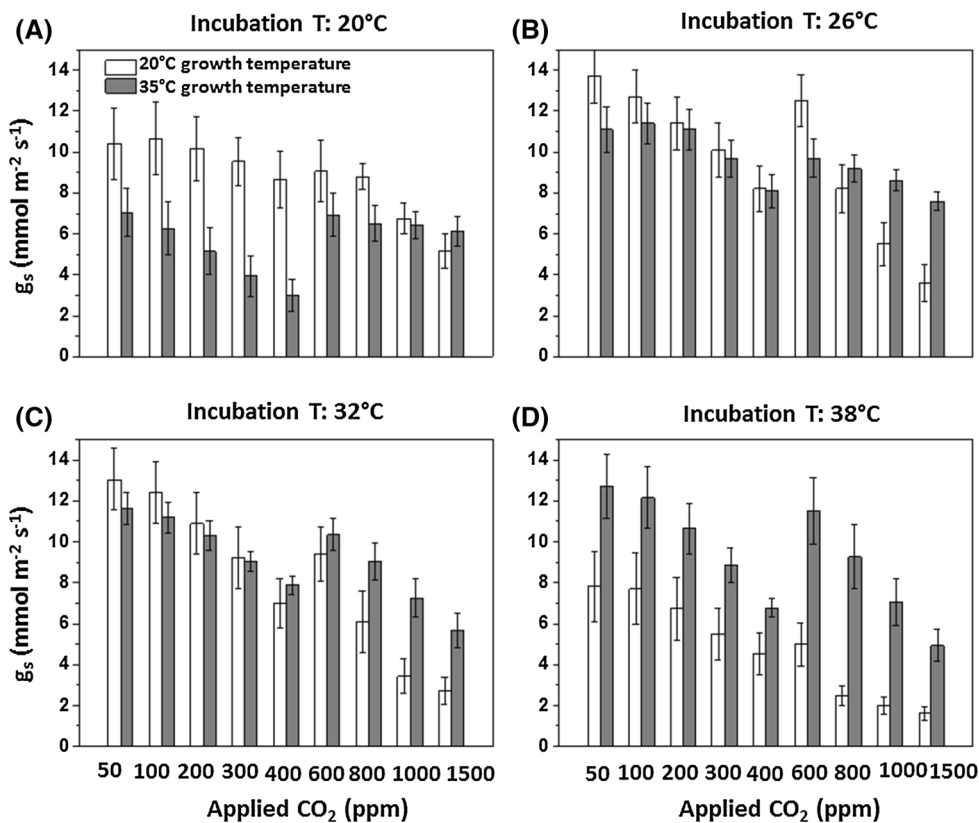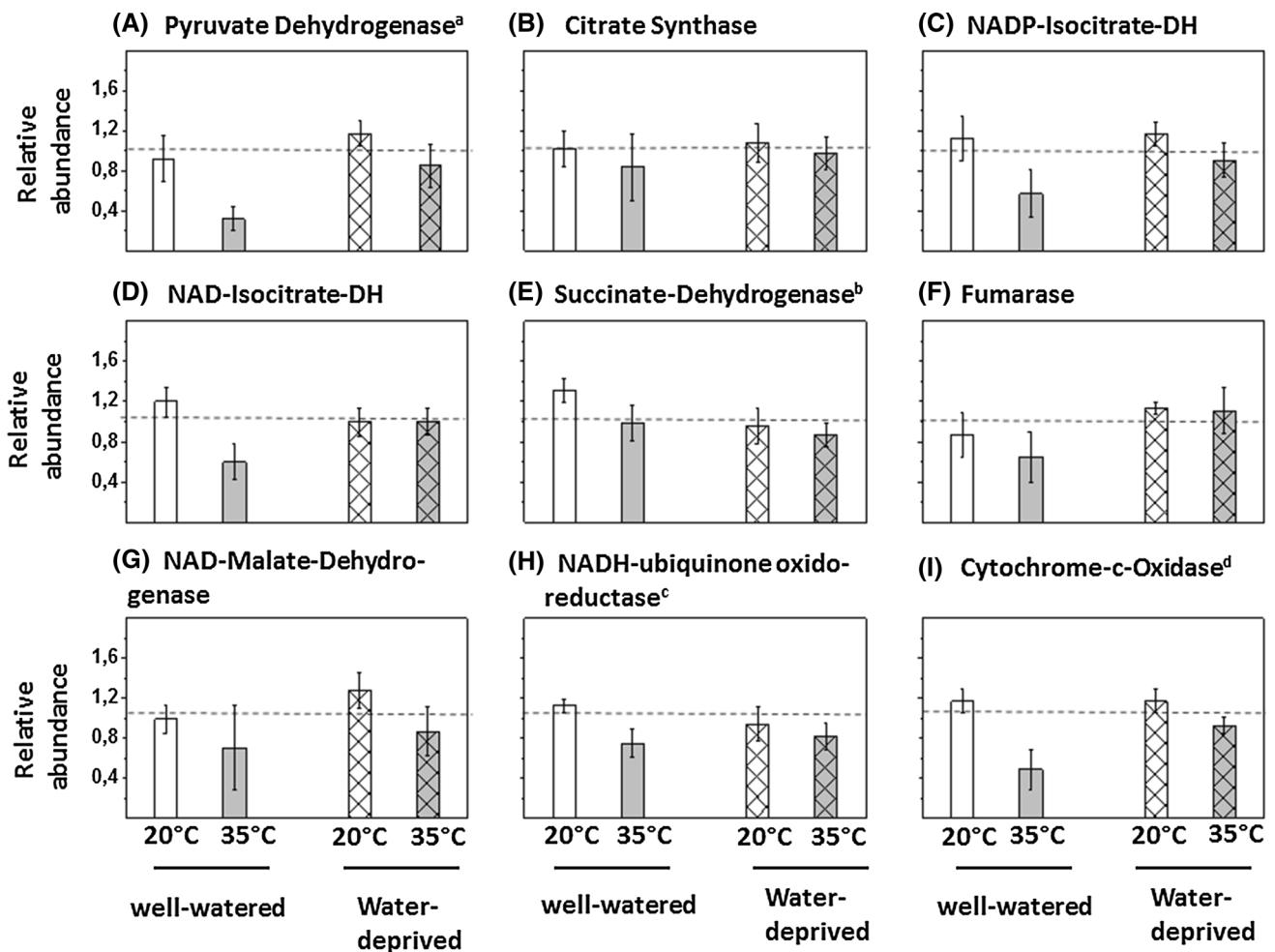
Fig. 8 Treatment effects on abundance of mitochondrial enzymes. **a** Pyruvate dehydrogenase ([a]complex dihydrolipoamide acetyltransferase; subunits α and β of complex e1 with similar patterns, not shown). **b** Citrate synthase. **c** NADP-dependent isocitrate dehydrogenase. **d** NAD-dependent isocitrate dehydrogenase. **e** Succinate dehydrogenase ([b]iron-protein subunit). **f** Fumarase. **g** NAD-dependent malate dehydrogenase. **h** NADH-ubiquinone oxidoreductase ([c]13 kDa-b-subunit; 20 kDa subunit and b14 subunit with similar patterns, not shown). **i** Cytochrome-c-oxidase ([d]subunit Vb). Each *column* shows the average $\pm$ SE of five independent replicates. Data were subjected to two-way ANOVA to assess the significance of growth temperature and water availability for abundance of individual proteins (see Table 3)

exposed to 35 °C for 2 weeks. These reductions in enzyme abundances were reversed by 4 days of water shortage at 35 °C (Table 3). Growth at 35 °C led to strong declines in Sucrose-P-Synthase (Fig. 5k), and Fructose-6P-2 Kinase-fructose-2,6-bisphosphate phosphatase (Fig. 5l; Table 3). Taken together, these results indicate reduced P_i regeneration capacity, but enhanced carboxylation capacity (V_{cmax}) under elevated growth temperature.

In an independent experiment, we tested the effects of growth temperature on V_{cmax} in well-watered plants. We found that V_{cmax} was slightly less for 35 °C grown plants than for 20 °C grown plants, when measured at 20 °C (Fig. 6a). The reverse pattern was observed at 38 °C (Fig. 6d). That is, temperature-dependent activation of Rubisco was a little more pronounced in 35 °C grown as compared with 20 °C grown plants (statistically not significant at $p < 0.05$). This effect is somewhat incongruous with the strong increase in Rubisco activase (for 35 °C grown plants). Stomatal conductance was greater for plants grown at 20 °C instead of 35 °C, when measured at 20 °C (Fig. 7a). The reverse pattern was again observed at an incubation temperature of 38 °C (Fig. 7d). Consequently, biochemical CO_2 demand and re-supply of CO_2 via stomata were closely coordinated, and responded in tandem to changed growth temperature.

Factors controlling the acclimation of respiration to heat and drought

Proteome analysis showed that reductions in respiratory capacity (R_{Cap}) in response to increased growth temperature were at least partly associated with reduced abundances of mitochondrial enzymes. Pyruvate dehydrogenase
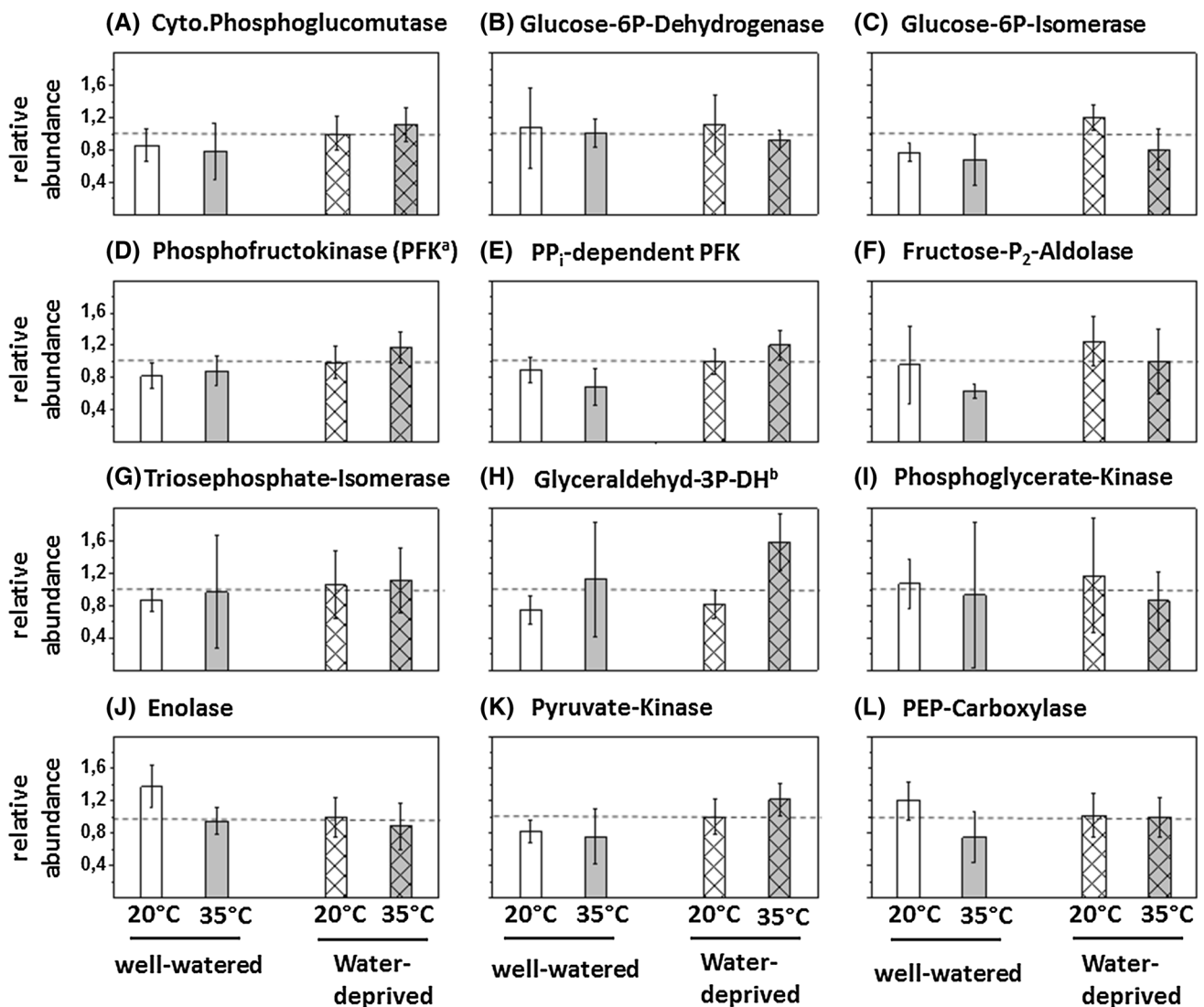
Fig. 9 Treatment effects on abundance of glycolytic enzymes. **a** Phosphoglucomutase. **b** Glucose-6P-dehydrogenase (oxidative pentose phosphate cycle). **c** Glucose-6P-isomerase. **d** Phosphofructokinase ([a]pfkb-type carbohydrate kinase family protein). **e** PP$_i$-dependent PFK. **f** Fructosebisphosphate-aldolase. **g** Triosephosphate-isomerase. **h** Glyceraldehyde-3P-dehydrogenase ([a]NAD-dependent isoform). **i** Phosphoglycerate-kinase. **j** Enolase. **k** Pyruvate kinase. **l** Phosphoenolpyruvate-carboxylase. Each *column* shows the average ± SE of five independent replicates. Data were subjected to two-way ANOVA to assess the significance of growth temperature and water availability for abundance of individual proteins. *N.s.* not significant

(Fig. 8a), NADP-isocitrate dehydrogenase (Fig. 8c), NAD-malate dehydrogenase (Fig. 8f), and cytochrome-*c*-oxidase (Fig. 8h) were reduced by 50–60% under well-watered conditions, but only by 20–30% after water deprivation. These effects were also revealed by significant interaction terms (i.e., $T \times D$ or growth temperature × water availability), similar to effects on total leaf-N (Table 3). Abundances of citrate synthase (Fig. 8b), succinate dehydrogenase (statistically not significant, Fig. 8e), fumarase (n.s., Fig. 8f), and NADH-ubiquinone oxidoreductase (Fig. 8g) were reduced by 20–30% under well-watered conditions, but only by 10–15% after water deprivation (Table 3).

Respiratory capacity may also depend on substrate supply to mitochondria. Glycolytic carbon flux is heavily dependent on formation of fructose-1,6-bisphosphate via phosphofructokinase, and by formation of pyruvate via pyruvate kinase (Givan 1999; Plaxton and Podesta 2006). Abundances of PFK (Fig. 9d, e), pyruvate kinase (Fig. 9k), and PEP-carboxylase (Fig. 9l) declined by 0–15% in response to increased growth temperatures under well-watered conditions, but *increased* with temperature when water was withdrawn (Table 3). These temperature and irrigation-induced patterns are qualitatively similar to patterns observed for mitochondrial enzymes, even though the temperature × water effect was more pronounced for
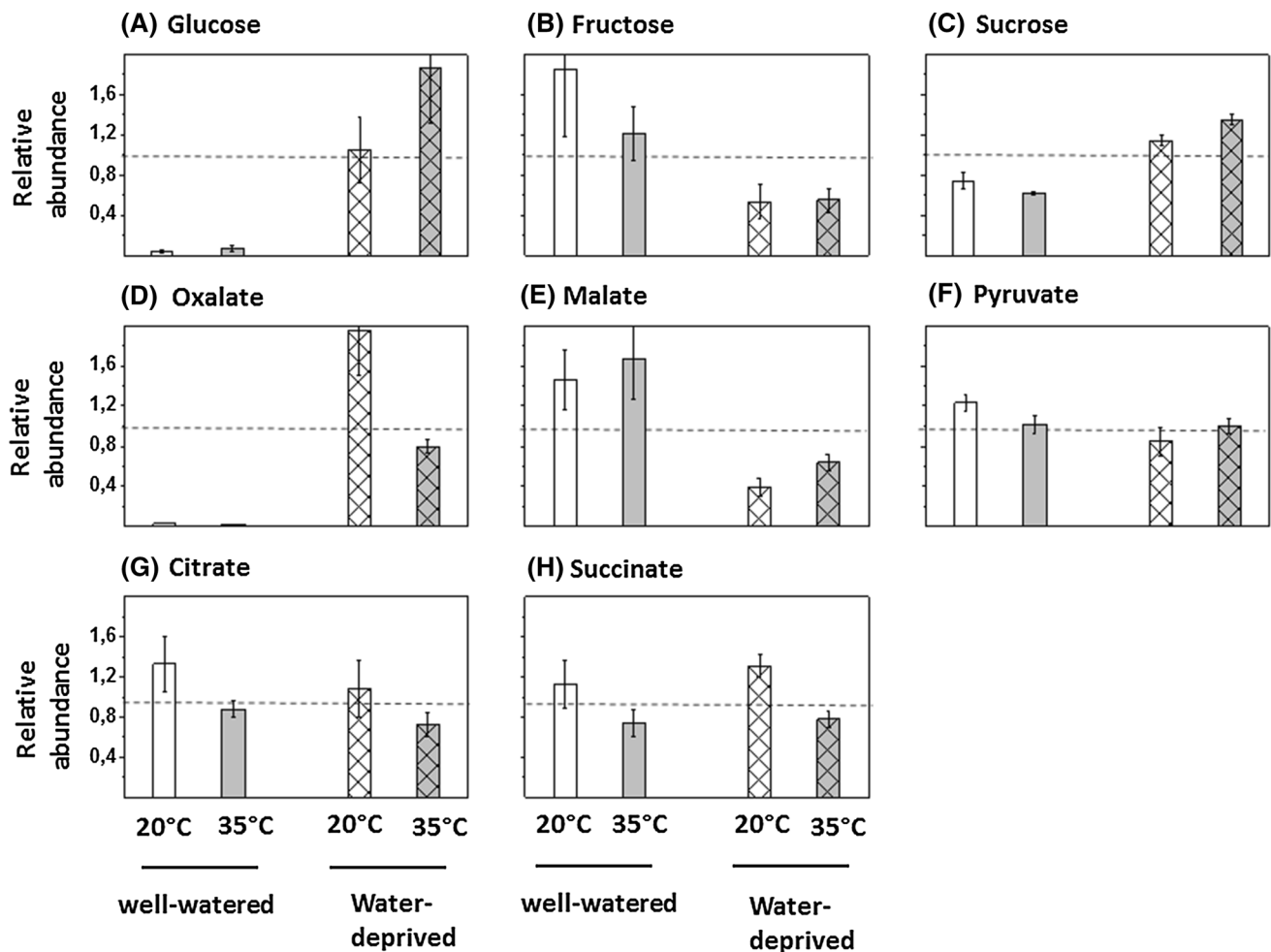
Fig. 10 Treatment effects on abundance of soluble carbohydrates and organic acids. **a** Glucose. **b** Fructose. **c** Sucrose. **d** Oxalate. **e** Malate. **f** Pyruvate. **g** Citrate. **h** Succinate. Each *column* shows the average ± SE of eight independent replicates. Data show relative variation between treatments based on leaf area. For results of statistical analysis see Table 3

mitochondrial than for glycolytic enzymes (PFK, pyruvate kinase, PEPC). Furthermore, many enzymes down-stream of PFK, i.e., Triosephosphate-Isomerase (Fig. 9g), glyceraldehyde-3P-dehydrogenase (Fig. 9h), or phosphoglycerate-kinase (Fig. 9i), were not significantly affected by growth temperature or water deprivation (Table 3).

Water deprivation significantly altered the balance between glucose and fructose (Fig. 10a, b), but had a little effect on abundances of enzymes involved in hexose metabolism, i.e., cytosolic phosphoglucomutase (Fig. 9a), glucose-6P-dehydrogenase (Fig. 9b), or glucose-6P-isomerase (Fig. 9c). Water deprivation significantly increased sucrose concentrations (Fig. 10c). High growth temperature reduced sucrose concentrations by c. 15% in well-watered plants, but *increased* sucrose concentrations by c. 15% in water-deprived plants (significant interaction of $T \times W$; Table 3). This interactive effect was qualitatively similar to those for glycolytic and mitochondrial enzymes.

Malates, and especially pyruvate, are known substrates for mitochondrial respiration. Malate concentrations were marginally greater at 35 °C than at 20 °C, but were strongly reduced by water deprivation (Fig. 10e; Table 3). Water deprivation had a little effect on pyruvate concentrations, but the $T \times W$-effect on pyruvate was similar to that observed for sucrose (Fig. 10f; Table 3). Growth at high temperature significantly reduced concentrations of the TCA-cycle intermediates citrate and succinate (Fig. 10g, h; Table 3).

Discussion

A/T curves of respiration and photosynthesis can be described by the same equation despite very different appearances

Algebraic models of the type used here to describe temperature responses of dark respiration and light-saturated

net CO_2 assimilation are useful across a range of species and growth conditions (e.g., Kruse et al. 2011; Noguchi et al. 2015). The value for comparative purposes (e.g., across treatments, species) of the parameters derived from such curve-fitting depends on their ability to robustly characterize underlying chemical, biochemical, and physical reactions. The parameter $E_o(Ref)$ captures initial increases in CO_2 exchange close to a low reference temperature, reflecting the activation energy of gas exchange at this reference temperature. This parameter is strongly correlated with the change of activation energy as incubation temperature increases (described by the δ-parameter). Close correlations between $E_o(Ref)$ and δ for both respiratory and photosynthetic temperature responses (Fig. 3) reflect common features of both processes, as well as their principal differences. For respiration, average δ_R was close to zero, so that respiratory temperature responses could, on average, be described by classical Arrhenius kinetics—giving rise to an exponential increase of CO_2 evolution between 20 and 45 °C incubation temperature. Individual R/T curves yielded δ_R values that were as often negative as positive, with an intercept of the correlation between δ_R and $E_o(Ref_R)$ at 54.5 kJ mol^{-1}. Similar results were recently obtained by Noguchi et al. (2015) and also by the previous studies using calorimetry to determine respiratory O_2 consumption (Kruse et al. 2008, 2012). While a mechanistic interpretation of the latter result was provided by Kruse et al. (2011), an interpretation is still required for the positive temperature sensitivity of E_{oRCO_2} and $\delta_{RCO_2} > 0$ (Noguchi et al. 2015).

For photosynthesis, δ_A was always negative, resulting in parabolic responses of photosynthesis to incubation temperature (Fig. 2b), with peak rates of net CO_2 assimilation at 30 ± 3 °C (Fig. 4l). The biological significance of close correlations between $E_o(Ref_A)$ and δ_A (Fig. 3a) is further elucidated and discussed in a companion study (Kruse et al. 2016).

We focus here on the other remarkable feature of A/T curves—their apparent symmetry. Reductions in rates of CO_2 assimilation above T_{opt} were more pronounced in water-deprived than in well-watered plants and apparently related to a stronger decline in stomatal conductance (Fig. 2c). It could be wrongly concluded that stomatal sensitivity to enhanced VPD (as incubation temperatures increases) was more pronounced in water-deprived plants, and that stomatal closure caused limitations of photosynthesis at incubation temperatures above T_{opt}. Such a conclusion would ignore symmetric responses of photosynthesis to temperature (see also Gunderson et al. 2010), despite asymmetrical changes in VPD. This symmetry remained despite acclimation to different water supply and growth temperature (Fig. 2e), suggesting that physiological processes underlying photosynthesis, namely

rates of carboxylation (A_C), rates of RuP$_2$-regeneration (A_J), rates of P_i regeneration, and supply of CO_2 to the chloroplasts are tightly coordinated—under steady-state conditions. Under the conditions and for the species of the present experiment, there was no consistent switch from one limiting process to another limiting process—with different temperature sensitivities—at some distinct incubation temperature.Instead

$$\frac{dE_{oA}}{dT_{Term}} = 2 \times \delta_A = \text{constant}, \qquad (9)$$

where $T_{Term} = \frac{T-T_{ref}}{T \times T_{ref}}$ (1000/K), and $\delta_A < 0$.

Any marginal increase in incubation temperature (T, in units of K) resulted in the same decline of E_{oA}. The validity of the above conclusion (i.e., Eq. 9) evidently depends on how 'smoothly' experimental data can be fitted to the three-parameter model (Eq. 6). Goodness of fits was somewhat lower for photosynthesis (average R^2: 0.95; Fig. 2e) than for dark respiration (average R^2: 0.976 (Fig. 1); but generally closer to 1.0 if more sensitive calorimetric methods are employed, Kruse et al. 2011). It is technically more demanding to obtain an average measure of cross-sectional leaf-temperature in the light than in the dark, owing to a temperature-gradient between upper, light-exposed cell layers, and lower cell layers experiencing evaporative cooling. Second, at 45 °C incubation, temperature leaf net photosynthesis (A) often approached zero or became negative, for which ln$A$ values are not defined. These technical and methodological limitations produce some random scatter around the line of best fit (least-square regression), which is unlikely of biological significance (also see Kruse et al. 2016). However, biologically significant departures from the modified Arrhenius equation are observable, if incubation temperatures exceed those to which plants are acclimated and/or adapted.

Temperate or boreal tree species, for example, frequently exhibit T_{opt} considerably lower than T_{opt} of date palm (30 ± 3 °C) (Berry and Björkman 1980). Application of incubation temperatures >35–40 °C can result in A/T curves becoming asymmetrical for such species (unpublished results). These changes may well be a result of limitations in V_{cmax}, J_{max}, or CO_2 supply at high incubation temperatures. Similarly, application of incubation temperatures <20 °C in this study might have resulted in limitations of A via insufficient P_i regeneration capacity, at least for 35 °C grown *P. dactylifera*.

Acclimation of photosynthesis to heat and drought

Acclimation to 35 °C reduced the biochemical capacity for P_i regeneration (Fig. 5k, l), *relative* to those for: (a) RuP$_2$ regeneration (Fig. 5a, d, e), and (b) carboxylation (Fig. 5b, c), without any effect on the temperature sensitivity of E_{oA}

at incubation temperatures between 20 and 45 °C. In particular, growth at elevated temperature markedly increased production of Rubisco activase (Fig. 5c). Rubisco activase is ideally suited to mediate between A_C and A_J, because its activity is regulated by the ATP/ADP ratio and redox state of chloroplasts (Portis 2003; Ruuska et al. 2000), and, thus, by thylakoid electron transport (Zhang et al. 2002; Sage and Kubien 2007; Yamori et al. 2014).

The pronounced increase in abundance of Rubisco activase in 35 °C grown plants only slightly increased V_{cmax} at 38 °C incubation temperature (Fig. 6d). Plants were cultivated at low light intensity (200 μmol quanta m^{-2} s^{-1}), and exhibited low photosynthetic capacity compared with other species or growth conditions (Wullschleger 1993). Despite increased abundance of Rubisco activase, its catalytic activity was apparently constrained by limitations in J_{max} and A_J. Similarly, A/T curves were conducted at 1200 μmol quanta m^{-2} s^{-1} (and ambient CO_2), and CO_2 assimilation of plants acclimated to low light was limited by J_{max} across the entire range of incubation temperatures—where A_J remained tightly coordinated with A_C and rates of P_i regeneration.

Acclimation to higher growth temperature also enhanced stomatal conductance at high incubation temperature (Fig. 7d), which suggests close coordination between biochemical capacity of A (J_{max} or V_{cmax}) and g_s. At high incubation temperature, stomatal conductance of 20 °C grown plants was particularly sensitive to increased CO_2 concentrations. As a result, substomatal [CO_2] did not exceed 600 ppm (Fig. 6e). At c_i between 300–600 ppm CO_2, photosynthesis is often co-limited by both A_C and A_J (Long and Bernacchi 2003; Sharkey et al. 2007), as another example of tight coordination between processes regulating biochemical demand, and CO_2 supply via stomata.

At current atmospheric [CO_2], Rubisco operates below its half-saturation constant for CO_2 fixation (K_C) (Siedow and Day 2000). The low catalytic efficiency of (active) Rubisco is compensated for by large amounts of Rubisco in chloroplasts (Warren and Adams 2004). Nonetheless, only a fraction of this enzyme pool exhibits active catalytic sites. It has long puzzled plant researchers that plant leaves contain a seemingly excessive amount of non-active Rubisco protein (Stitt and Schulze 1994; Warren and Adams 2004; Yamori et al. 2011). In combination with variable amounts of Rubisco activase, maintenance of a large pool of Rubisco proteins may confer greater flexibility to induction of the photosynthetic machinery. While variable abundance of Rubisco activase has a little effect on steady-state rates of light-saturated photosynthesis per se (Yamori and von Caemmerer 2009), Yamori et al. (2012) recently demonstrated that abundance of Rubisco activase was correlated with the speed of photosynthetic light-induction.

This study demonstrated that temperature is an environmental cue for stimulation of synthesis of Rubisco activase (Fig. 5c), even under the relatively low light conditions in our growth chambers. P. dactylifera is adapted to a hot and sunny environment, where air and leaf-temperatures vary with incoming solar radiation. We interpret enhanced synthesis of Rubisco activase in 35 °C grown plants (Crafts-Brandner and Salvucci 2000; Salvucci and Crafts-Brandner 2004), as helping counteract risks of oxidative stress under high light. In addition to serving as a storage pool for nitrogen (Warren et al. 2003), maintenance of 'excess' Rubisco-protein may act as a safety buffer allowing, in combination with increased Rubisco activase abundance, for swift induction of CO_2 assimilation in response to changing light interception—such that production of reactive oxygen species and oxidative stress are avoided (Posch et al. 2008).

Water shortages had a little effect on A_{opt} and g_s at T_{opt} (Figs. 3c, 4d), but did affect the temperature sensitivity of E_{oA} (i.e., δ_A; Fig. 4j). P. dactylifera is a slow-growing species with conservative water usage, and short-duration water shortages (as applied here) were not sufficient to induce severe stress or stomatal closure. Nevertheless, imposed water shortage had clear-cut effects on carbohydrate utilization, partly via reversing the decline in abundance of ADP-glucose pyrophosphorylase caused by growth at greater temperatures (Fig. 5i). ADP-glucose pyrophosphorylase helps regulate starch synthesis. Water shortages also led to increased sucrose concentrations (Fig. 10c). Physiological processes controlling cell division and cell wall expansion in meristematic tissue are sensitive to alterations of the plant water status, long before any effects on stomatal conductance become apparent (Muller et al. 2011; Tardieu et al. 2011; Körner 2013; Fatichi et al. 2014). Slowing of growth (after 4–7 days of water deprivation) was associated with accumulation of carbohydrates, but not with down-regulation of A_{opt} or A_{growth} (Fig. 4h). It remains unknown if, or how, altered balance of triosephosphate utilization for starch synthesis, sucrose synthesis, or mitochondrial light respiration, is related to δ_A (but see Kruse et al. 2016).

Acclimation of dark respiration to heat and drought

Two weeks of acclimation to higher temperature strongly reduced physiological capacities of respiration (R_{Cap}, Fig. 4c) ('Type II' acclimation'), but produced a little change in $E_o(Ref_R)$ or δ_R (Fig. 4e, i) ('Type I' acclimation). For these reasons, changes in R_{Cap} and R_{ref} were similar, with significant reductions of R_{ref} in 35 °C grown plants (Fig. 4a). Nonetheless, significant 'Type II'

acclimation in *P. dactylifera* did not result in complete homeostasis of respiration at contrasting growth temperature, since R_{growth} remained greater in 35 °C grown than in 20 °C grown plants (Fig. 4g). Growth temperature-related shifts in $E_o(\text{Ref}_R)$ or δ_R (type I acclimation) are associated with shifts in metabolic flux mode, and may be the first part of an overall acclimation response (at the scale of hours to days, Atkin and Tjoelker 2003). This type of acclimation is significant for many herbaceous and crop species, and results in homeostasis of E_{oR} at contrasting growth temperature (i.e. $E_o(\text{Growth}_R)$; Noguchi et al. 2015). In this study, acclimation of *P. dactylifera* was mainly driven by reductions in R_{Cap} and we argue that 'type II' acclimation is a corollary of optimization of the efficiency of resource-use.

At higher growth temperature, large physiological capacity of source-leaf respiration, as derived from gas exchange measurements, offers a little advantage. ATP consumption by growth supporting processes, and plant growth itself, does not increase in proportion to the capacity of ATP supply. A large share of respiratory energy, transiently stored in ATP, is consumed by sucrose synthesis and by phloem loading of sucrose and amino acids, to support sink activity (Kruse et al. 2011). In this study, we recorded declines in abundances of sucrose-P-synthase (SPS) and fructose-6P-2 kinase-fructose-2,6-bisphosphate phosphatase (Fig. 5k, l), and in those of mitochondrial enzymes at high growth temperature (Fig. 8). Fructose-6P-2 kinase-fructose-2,6-bisphosphate phosphatase is a unique bi-functional enzyme with complex regulation, which is confined to the cytosol. It catalyzes both synthesis and cleavage of fructose-2,6-bisphosphate, which is key to the regulation of sucrose synthesis (Stitt 1990). High concentrations of this regulatory metabolite inhibit fructose-1,6-bisphosphate phosphatase and hence carbon flux into the hexose phosphate pool for sucrose synthesis (Buchanan et al. 2000). We interpret reduced abundances of both fructose-6P-2 kinase and SPS as reflecting reduced *biochemical* capacity for enzymatic catalysis that remains sufficient to regulate fructose-2,6-bisphosphate and sucrose synthesis (with comparatively high Q_{10}; Stitt and Grosse 1988; Strand et al. 1999) at high growth temperature.

Growth at high temperatures provides plants with the opportunity to reduce investment of nitrogen into the mitochondrial machinery and reallocate N elsewhere (Fig. 4k). As a result, energy costs (ATP) for the maintenance of unnecessarily large enzyme pools are reduced under elevated growth temperature (Atkin et al. 2005a, b). Comparatively, large reductions of mitochondrial enzymes were recorded for well-watered plants (Fig. 8). Although reductions were much less pronounced in water-deprived plants, their *physiological* capacity at high growth temperature was only marginally greater compared with well-watered plants (Fig. 4c). This was not the result of limited pyruvate availability for mitochondrial respiration per se (Fig. 10f). In fact, abundances of key enzymes for the regulation of glycolysis like PFK (Fig. 9d, e), pyruvate kinase (Fig. 9k), and PEPC (Fig. 9l) were greater in water-deprived than in well-watered plants, when grown at 35 °C. Increased biochemical capacity of water-deprived plants ensures that on cessation of 'drought', accumulated carbohydrates can swiftly be remobilized and exported via swift induction of ATP-synthesis, unconstrained by limitations of biochemical capacity of mitochondria (cf. Smith and Stitt 2007).

Plants develop different strategies to optimize resource-use efficiency according to their adapted ecological niche. It is, perhaps, unsurprising that the degree (and Type) of respiratory acclimation greatly varies between species (Larigauderie and Körner 1995; Tjoelker et al. 1999; Bunce 2000; Loveys et al. 2002; Kruse et al. 2012; Slot and Kitajima 2015; Noguchi et al. 2015). Our results support reports that respiratory temperature acclimation is comparatively swift (Bolstad et al. 2003; Lee et al. 2005; Campbell et al. 2007), whereas acclimation of photosynthetic capacity often appears less responsive (Ow et al. 2010; Chi et al. 2013). Nonetheless, the ratio of A_{growth}/R_{growth} remained close to constant in this study, suggesting that acclimation of photosynthetic CO_2 assimilation and respiratory CO_2 loss was causally linked.

Concluding remarks

Many plants must cope with temperature regimes that encompass variation of more than 20 °C, at scales from as short as one day, to years. A/T curves help characterization of thermal acclimation, albeit we lack a standard approach to interpretation (but see companion study Kruse et al. 2016). We used a modified Arrhenius equation as a tool to identify transition temperatures that might indicate shifts between rate-limiting processes of A. The apparent constancy of dE_{oA}/dT, and strong relations between parameters $E_o(\text{Ref}_A)$ and δ_A, suggest tight coordination of physiological processes underlying photosynthesis—at least between 20–45 °C incubation temperatures applied to date palm. A/T curves remained symmetrical under elevated growth temperature (and water shortage) despite large shifts between biochemical capacities for triosephosphate utilization relative to RuP_2 carboxylation. Growth at elevated temperature significantly reduced the physiological capacity of respiration (R_{Cap}), which was, in part, resulting from reduced abundances of some key-regulatory enzymes of respiration in well-watered plants. Temperature-induced reduction of biochemical capacity

was less for water-deprived plants, but R_{Cap} remained low. We anticipate further application of the three-parameter model (more species, greater range of environmental conditions; Kruse et al. 2016) will significantly help development of a deeper mechanistic understanding of acclimation processes, and of energy conservation via respiration and photosynthesis.

Author contribution statement JöK designed the experiment; JöK, GD, LA, JüK and WS performed measurements; JöK statistically analyzed the data; JöK, MAA, SA and HR wrote the paper.

References

Amthor JF (2010) From sunlight to phytomass: on the potential efficiency of converting solar radiation to phyto-energy. New Phytol 188:939–959

Armstrong AF, Logan DC, Tobin AK, O'Toole P, Atkin OK (2006) Heterogeneity of plant mitochondrial responses underpinning respiratory acclimation to the cold in *Arabidopsis thaliana* leaves. Plant Cell Environ 29:940–949

Atkin OK, Macherel D (2009) The crucial role of plant mitochondria in orchestrating drought tolerance. Ann Bot 103:581–597

Atkin OK, Tjoelker MG (2003) Thermal acclimation and the dynamic response of plant respiration to temperature. Trends Plant Sci 8(7):343–351

Atkin OK, Bruhn D, Hurry VM, Tjoelker MG (2005a) Evans Review No. 2. The hot and the cold: unraveling the variable response of plant respiration to temperature. Funct Plant Biol 32:87–105

Atkin OK, Bruhn D, Tjoelker MG (2005) Response of plant respiration to changes in temperature: mechanisms and consequences of variations in Q_{10} values and acclimation. In: Lambers H, Ribas-Carbo M (eds) Plant respiration, pp 95–135

Atkin OK, Bloomfield KJ, Reich PB, Tjoelker MG, Asner GP, Bonal D, Bönisch G et al (2015) Global variability in leaf respiration in relation to climate, plant functional types and leaf trait. New Phytol. doi:10.1111/nph.13253

Atkins PW, de Paula J (2006) Physikalische Chemie. Wiley-VCH, Weinheim

Battaglia M, Beadle C, Loughhead S (1996) Photosynthesis temperature response of *Eucalyptus globulus* and *Eucalyptus nitens*. Tree Physiol 16:81–89

Bernacchi CJ, Singsaas EL, Pimentel C, Portis AR, Long SP (2001) Improved temperature response functions for models of Rubisco-limited photosynthesis. Plant Cell Environ 24:253–259

Bernacchi CJ, Bagley JE, Serbin SP, Ruiz-Vera UM, Rosenthal DM, Vanloocke A (2013) Modelling C_3 photosynthesis from the chloroplast to the ecosystem. Plant Cell Environ 36:1641–1657

Berry JA, Björkman O (1980) Photosynthetic response and adaptation to temperature in higher plants. Annu Rev Plant Physiol 31:491–543

Bolstad PV, Reich P, Lee T (2003) Rapid temperature acclimation of leaf respiration rates in *Quercus alba* and *Quercus rubra*. Tree Physiol 23:969–976

Bruhn D, Egerton JJG, Loveys BR, Ball MC (2007) Evergreen leaf respiration acclimates to long-term nocturnal warming under field conditions. Global Change Biol 13:1216–1223

Buchanan BB, Gruissem W, Jones RL (2000) Biochemistry and molecular biology of plants. American Society of Plant Physiologists, Rockville

Bunce JA (2000) Acclimation of photosynthesis to temperature in eight cold and warm climate herbaceous C_3 species: temperature dependence of parameters of a biochemical photosynthesis model. Photosynth Res 53:59–67

Bunce JA (2007) Direct and acclimatory responses of dark respiration and translocation to temperature. Ann Bot 100:67–73

Campbell C, Atkinson L, Zaragoza-Castells J, Lundmark M, Atkin O, Hurry V (2007) Acclimation of photosynthesis and respiration is asynchronous in response to changes in temperature regardless of plant functional group. New Phytol 176:375–389

Cannell MGR, Thornley JHM (2000) Modeling plant respiration: some guiding principles. Ann Bot 85:45–54

Chi Y, Xu M, Shen R, Yang Q, Huang Q, Wan S (2013) Acclimation of foliar respiration and photosynthesis in response to experimental warming in a temperate steppe in Northern China. PLoS One 8:1–13

Clarke A (2006) Temperature and the metabolic theory of ecology. Funct Ecol 20:405–412

Cox J, Mann M (2008) MaxQuant enables high peptide identification rates, individualized p.p.b.-range mass accuracies and proteome-wide protein quantification. Nat Biotechnol 26:1367–1372

Cox J, Neuhauser N, Michalski A, Scheltema RA, Olsen JV, Mann M (2011) Andromeda: a peptide search engine integrated into the MaxQuant environment. J Proteome Res 10:1794–1805

Crafts-Brandner SJ, Salvucci ME (2000) Rubisco activase constrains the photosynthetic potential of leaves at high temperature and CO_2. Proc Natl Acad Sci USA 97:13430–13435

Dewar RC, Medlyn BE, McMurtrie RE (1999) Acclimation of the respiration/photosynthesis ratio to temperature: insights from a model. Global Change Biol 5:615–622

Diaz-Espejo A (2013) New challenges in modelling photosynthesis: temperature dependencies of Rubisco kinetics. Plant Cell Environ 36:2104–2107

Dillaway D, Kruger EL (2010) Thermal acclimation of photosynthesis: a comparison of boreal and temperate tree species along a latitudinal transect. Plant Cell Environ 33:888–899

Dreyer E, Le Roux X, Montpied P, Daudet FA, Masson F (2001) Temperature response of leaf photosynthetic capacity in seedlings from seven temperature tree species. Tree Physiol 21:223–232

Farquhar GD, von Caemmerer S, Berry JA (1980) A biochemical model of photosynthetic CO_2 assimilation in leaves of C_3 species. Planta 149:78–90

Fatichi S, Leutzinger S, Körner C (2014) Moving beyond photosynthesis: from carbon source to sink-driven vegetation modeling. New Phytol 201:1086–1095

Flexas J, Bota J, Galmés J, Medrano H, Ribas-Carbó M (2006) Keeping a positive carbon balance under adverse conditions: responses of photosynthesis and respiration to water stress. Physiol Plant 127:343–352

Gifford RM (2003) Plant respiration in productivity models: conceptualization, representation and issues for global terrestrial carbon-cycle research. Funct Plant Biol 30:171–186

Givan CV (1999) Evolving concepts in plant glycolysis: two centuries of progress. Biol Rev 74:277–309

Gunderson CA, O'Hara KH, Campion CM, Walker AW, Edwards NT (2010) Thermal plasticity of photosynthesis: the role of acclimation in forest responses to a warming climate. Global Change Biol 16:2272–2286

Guy CL, Huber JLA, Huber SC (1992) Sucrose phosphate synthase and sucrose accumulation at low temperature. Plant Physiol 99:1443–1448

Hikosaka K, Ishikawa K, Borjigidai A, Muller O, Onoda Y (2006) Temperature acclimation of photosynthesis: mechanisms involved in the change in temperature dependence of photosynthetic rate. J Exp Bot 57:291–302

Hurry VM, Strand Å, Tobiæson M, Gardeström P, Öquist G (1995) Cold hardening of spring and winter wheat and rape results in differential effects on growth, carbon metabolism, and carbohydrate content. Plant Physiol 109:697–706

Hüve K, Bichele I, Rasulov B, Niinemets Ü (2011) When it is too hot for photosynthesis: heat-induced instability of photosynthesis in relation to respiratory burst, cell permeability changes and H_2O_2 formation. Plant Cell Environ 34:113–126

Kattge J, Knorr W (2007) Temperature acclimation in a biochemical model of photosynthesis: a reanalysis of data from 36 species. Plant Cell Environ 30:1176–1190

Kirschbaum MUF, Farquhar GD (1984) Temperature dependence of whole-leaf photosynthesis in *Eucalyptus pauciflora* Sieb. ex Spreng. Aust J Plant Physiol 11:519–538

Kopka J, Schauer N, Krueger S, Birkemeyer C, Usadel B, Bergmuller E, Dormann P, Weckwerth W, Gibon Y, Stitt M, Willmitzer L, Fernie AR, Steinhauser D (2005) GMD@CSB.DB: the Golm Metabolome Database. Bioinformatics 21:1635–1638

Körner C (2013) Growth controls photosynthesis—mostly. Nova Acta Leopold 114:273–283

Kreuzwieser J, Hauberg J, Howell KA, Carroll A, Rennenberg H, Millar AH, Whelan J (2009) Differential response of gray poplar leaves and roots underpins stress adaptation during hypoxia. Plant Physiol 149:461–473

Kruse J, Adams MA (2008a) Sensitivity of respiratory metabolism and efficiency to foliar nitrogen during growth and maintenance. Global Change Biol 14:1233–1251

Kruse J, Adams MA (2008b) Three parameters comprehensively describe the temperature response of respiratory oxygen reduction. Plant Cell Environ 31:954–967

Kruse J, Adams MA (2008c) Integrating two physiological approaches helps relate plant respiration to growth of *Pinus radiata*. New Phytol 180:841–852

Kruse J, Hopman P, Adams MA (2008) Temperature responses are a window to the physiology of dark respiration: differences between CO_2 release and O_2 reduction shed light on energy conservation. Plant Cell Environ 31:901–914

Kruse J, Rennenberg H, Adams MA (2011) Steps towards a mechanistic understanding of respiratory temperature responses. New Phytol 189:659–677

Kruse J, Turnbull T, Adams MA (2012) Disentangling respiratory acclimation and adaptation to growth temperature by *Eucalyptus* spp. New Phytol 195:149–163

Kruse J, Simon J, Rennenberg H (2013) Soil respiration and soil organic matter decomposition in response to climate change. In: Mattyssek R, Clarke N, Cudlin P, Mikkelsen TN, Tuovinen J-P, Wieser G, Paoletti E (eds) Climate change, air pollution and global challenges, pp 131–149

Kruse J, Alfarraj S, Rennenberg H, Adams MA (2016). A novel mechanistic interpretation of instantaneous temperature responses of leaf net photosynthesis. Photosynth Res. doi:10.1007/s11120-016-0262-x

Kurimoto K, Day DA, Lambers H, Noguchi K (2004) Effect of respiratory homeostasis on plant growth in cultivars of wheat and rice. Plant Cell Environ 27:853–862

Lambers H, Chapin FS, Pons TL (1998) Plant physiological ecology. Springer, New York

Larigauderie A, Körner C (1995) Acclimation of leaf dark respiration to temperature in alpine and lowland plant species. Ann Bot 76:245–252

Lee TD, Reich PB, Bolstad PV (2005) Acclimation of leaf respiration to temperature is rapid and related to specific leaf area, soluble

sugars and leaf nitrogen across three temperate deciduous tree species. Funct Ecol 19:640–647

Leegood RC, Edwards GE (1996) Carbon metabolism and photorespiration: temperature dependence in relation to other environmental factors. In: Baker NR (ed) Photosynthesis and the environment. Kluwer Academic, Dordrecht, pp 191–221

Lin Y-S, Medlyn BE, Ellsworth DS (2012) Temperature responses of leaf net photosynthesis: the role of component processes. Tree Physiol 32:219–231

Lloyd J, Taylor JA (1994) On the temperature dependence of soil respiration. Funct Ecol 8:315–323

Long SP, Bernacchi CJ (2003) Gas exchange measurements, what can they tell us about the underlying limitations to photosynthesis? Procedures and sources of error. J Exp Bot 54:2393–2401

Loveys BR, Scheurwater I, Pons TL, Fitter AH, Atkin OK (2002) Growth temperature influences the underlying components of relative growth rate: an investigation using inherently fast- and slow-growing plant species. Plant Cell Environ 25:975–987

Maseyk K, Grünzweig JM, Rotenberg E, Yakir D (2008) Respiration acclimation contributes to high carbon-use efficiency in a seasonally dry pine forest. Global Change Biol 14:1553–1567

Medlyn BE, Dreyer E, Ellsworth D, Harley PC, Kirschbaum MUF, Le Roux X, Montpied P, Strassmeyer J, Walcroft A, Wang K, Loustau D (2002) Temperature response of parameters of a biochemically based model of photosynthesis. II. A review of experimental data. Plant Cell Environ 25:1167–1179

Miroslavov EA, Kravkina IM (1991) Comparative analysis of chloroplasts and mitochondria in leaf chlorenchyma from mountain plants grown at different altitudes. Ann Bot 68:195–200

Muller B, Pantin F, Genard M, Turc O, Freixes S, Piques M, Gibon Y (2011) Water deficits uncouple growth from photosynthesis, increase C content, and modify the relationships between C and growth in sink organs. J Exp Bot 62:1715–1729

Noguchi K, Yamori W, Hikosaka K, Terashima I (2015) Homeostasis of the temperature sensitivity of respiration over a range of growth temperatures indicated by a modified Arrhenius model. New Phytol. doi:10.1111/nph.13339

O'Sullivan OS, Weerasinghe KWLK, Evans JR, Egerton JJG, Tjoelker MG, Atkin OK (2013) High-resolution temperature responses of leaf respiration in snow gum (*Eucalyptus pauciflora*) reveal high-temperature limits to respiratory function. Plant Cell Environ 36:1268–1284

Ow LF, Whitehead D, Walcroft AS, Turnbull MH (2010) Seasonal variation in foliar carbon exchange in *Pinus radiata* and *Populus deltoides*: respiration acclimates fully to changes in temperature but photosynthesis does not. Global Change Biol 16:288–302

Plaxton WC, Podesta FE (2006) The functional organization and control of plant respiration. Crit Rev Plant Sci 25:159–198

Portis AR Jr (2003) Rubisco activase: rubisco's catalytic chaperone. Photosynth Res 75:11–27

Posch S, Warren CR, Kruse J, Guttenberger H, Adams MA (2008) Nitrogen allocation and the fate of absorbed light in 21-year-old *Pinus radiata*. Tree Physiol 28:375–384

Pyl E-T, Piques M, Ivakov A, Schulze W, Ishihara H, Stitt M, Sulpice R (2012) Metabolism and growth in *Arabidopsis* depend on the daytime temperature but are temperature-compensated against cool nights. Plant Cell 24:2443–2469

Rappsilber J, Ishihama Y, Mann M (2003) Stop and go extraction tips for matrix-assisted laser desorption/ionization, nanoelectrospray, and LC/MS sample pretreatment in proteomics. Anal Chem 75:663–670

Rennenberg H, Loreto F, Polle A et al (2006) Physiological responses of forest trees to heat and drought. Plant Biology 8:556–571

Rodriguez-Calcerrada J, Atkin OK, Robson M, Zaragoza-Castells J, Gil L, Aranda I (2009) Thermal acclimation of leaf dark

respiration of beech seedlings experiencing summer drought in high and low light environments. Tree Physiol 30:214–224

Ruuska SA, Andrews TJ, Badger MR, Price GD, von Caemmerer S (2000) The role of chloroplast electron transport and metabolites in modulating rubisco activity in tobacco. Insights from transgenic plants with reduced amounts of cytochrome b/f complex or glyceraldehyde 3-phosphate dehydrogenase. Plant Physiol 122:491–504

Sage RF, Kubien DS (2007) The temperature response of C_3 and C_4 photosynthesis. Plant Cell Environ 30:1086–1106

Salvucci ME, Crafts-Brandner SJ (2004) Inhibition of photosynthesis by heat stress: the activation state of Rubisco as a limiting factor in photosynthesis. Physiol Plant 120:179–186

Schauer N, Steinhauser D, Strelkov S et al (2005) GC-MS libraries for the rapid identification of metabolites in complex biological samples. FEBS Lett 579:1332–1337

Seemann JR, Berry JA, Downton WJ (1984) Photosynthetic response and adaptation to high temperature in desert plants. Plant Physiol 75:364–368

Sharkey TD, Bernacchi CJ, Farquhar GD, Singsaas EL (2007) Fitting photosynthetic carbon dioxide response curves for C_3 leaves. Plant Cell Environ 30:1035–1040

Siedow JA, Day DA (2000) Respiration and photorespiration. In: Buchanan BB, Gruissem W, Jones RL (eds) Biochemistry and molecular biology of plants. American Society of Plant Physiologists, Rockville, pp 676–728

Slayter RO (1977) Altitudinal variation in the photosynthetic characteristics of snow gum, Eucalyptus pauciflora Sieb. ex Spreng. IV. Temperature response of four populations grown at different temperatures. Aust J Plant Physiol 4:583–594

Slot M, Kitajima K (2015) General patterns of leaf respiration to elevated temperatures across biomes and plant types. Oecologia 177:885–900

Smith NG, Dukes JS (2013) Plant respiration and photosynthesis in global-scale models: incorporating acclimation to temperature and CO_2. Global Change Biol 15:308–314

Smith AM, Stitt M (2007) Coordination of carbon supply and plant growth. Plant Cell Environ 30:1126–1149

Stitt M (1990) Fructose 2,6-bisphosphate as a regulatory metabolite in plants. Annu Rev Plant Physiol Plant Mol Biol 41:153–185

Stitt M, Grosse H (1988) Interactions between sucrose synthesis and CO_2 fixation. IV. Temperature-dependent adjustment of the relation between sucrose synthesis and CO_2-fixation. J Plant Physiol 133:392–400

Stitt M, Hurry V (2002) A plant for all seasons: alterations in photosynthetic carbon metabolism during cold acclimation in Arabidopsis. Curr Opin Plant Biol 5:199–206

Stitt M, Schulze E-D (1994) Does Rubisco control the rate of photosynthesis and plant growth? An exercise in molecular ecophysiology. Plant Cell Environ 17:465–487

Strand Å, Hurry VM, Henkes S, Huner NPA, Gustaffsson P, Gardeström P et al (1999) Acclimation of Arabidopsis leaves developing at low temperatures. Increasing cytoplasmic volume accompanies increased activities of enzymes in the Calvin cycle and in the sucrose-biosynthesis pathway. Plant Physiol 119:1387–1397

Tardieu F, Granier C, Muller B (2011) Water deficit and growth. Co-ordinating processes without an orchestrator? Curr Opin Plant Biol 14:283–289

Tengberg M (2003) Research into the origins of date palm domestication. The date palm: from traditional resource to Green Wealth. The Emirates Center for Strategic Studies and Research, Abu Dhabi, pp 51–62

Thornley JHM (2011) Plant growth and respiration re-visited: maintenance respiration defined—it is an emergent property of, not a separate process within, the system—and why the respiration: photosynthesis ratio is conservative. Ann Bot 108:1365–1380

Tjoelker MG, Oleksyn J, Reich PB (1999) Acclimation of respiration to temperature and CO_2 in seedlings of boreal tree species in relation to plant size and relative growth rate. Global Change Biol 49:679–691

Tjoelker MG, Oleksyn J, Reich PB (2001) Modelling respiration of vegetation: evidence for a general temperature-dependent Q_{10}. Global Change Biol 7:223–230

Von Caemmerer S (2013) Steady-state models of photosynthesis. Plant Cell Environ 36:1617–1630

Von Caemmerer S, Evans JR (2015) Temperature responses of mesophyll conductance differ greatly between species. Plant Cell Environ 38:629–637

Walker B, Ariza LS, Kaines S, Badger MR, Cousins AB (2013) Temperature response of in vivo Rubisco kinetics and mesophyll conductance in Arabidopsis thaliana: comparisons to Nicotiana tabacum. Plant Cell Environ 36:2108–2119

Warren CR (2008) Does growth temperature affect the temperature responses of photosynthesis and internal conductance to CO_2? A test with Eucalyptus regnans. Tree Physiol 28:11–19

Warren CR, Adams MA (2004) Evergreen trees do not maximize instantaneous photosynthesis. Trends Plant Sci 9:270–274

Warren CR, Dreyer E (2006) Temperature response of photosynthesis and internal conductance to CO_2: results from two independent approaches. J Exp Bot 57:3057–3067

Warren CR, Dreyer E, Adams MA (2003) Photosynthesis-Rubisco relationships in foliage of Pinus sylvestris in response to nitrogen supply and the proposed role of Rubisco and amino acids as nitrogen stores. Trees Struct Funct 17:359–366

Way DA, Yamori W (2014) Thermal acclimation of photosynthesis: on the importance of adjusting our definitions and accounting for thermal acclimation of respiration. Photosynth Res 119:89–100

Weih M, Karlsson PS (2001) Growth response of mountain birch to air and soil temperature: is increasing leaf-nitrogen content an acclimation to lower air temperature? New Phytol 150:147–155

Wullschleger SD (1993) Biochemical limitations to carbon assimilation in C_3 plants—a retrospective analysis of the A/C_i curves from 109 species. J Exp Bot 44:907–920

Xu CY, Griffin KL (2006) Seasonal variation in the temperature response of leaf respiration in Quercus rubra: foliage respiration and leaf properties. Funct Ecol 20:778–789

Yamasaki T, Yamakawa T, Yamane Y, Koike H, Satoh K, Katoh S (2002) Temperature acclimation of photosynthesis and related changes in photosystem II electron transport in winter wheat. Plant Physiol 128:1087–1097

Yamori W, von Caemmerer S (2009) Effect of Rubisco activase deficiency on the temperature response of CO_2 assimilation rate and Rubisco activation state: insights from transgenic tobacco with reduced amounts of Rubisco activase. Plant Physiol 151:2073–2082

Yamori W, Noguchi K, Terashima I (2005) Temperature acclimation of photosynthesis in spinach leaves: analyses of photosynthetic components and temperature dependencies of photosynthetic partial reactions. Plant Cell Environ 28:536–547

Yamori W, Nagai T, Makino A (2011) The rate-limiting step for CO_2 assimilation at different temperatures is influenced by the leaf nitrogen content in several C_3 crop species. Plant Cell Environ 34:764–777

Yamori W, Masumoto C, Fukayama H, Makino A (2012) Rubisco activase is a key regulator of non-steady state photosynthesis at any leaf temperature and to a lesser extent, of steady-state photosynthesis at high temperature. Plant J 71:871–880

Yamori W, Hikosaka K, Way DA (2014) Temperature response of photosynthesis in C_3, C_4 and CAM plants: temperature

acclimation and temperature adaptation. Photosynth Res 119:101–117

Zauber H, Schulze WX (2012) Proteomics wants cRacker: automated standardized data analysis of LC/MS derived proteomic data. J Proteome Res 11:5548–5555

Zhang N, Kallis RP, Ewy RG, Portis AR Jr (2002) Light modulation of Rubisco in Arabidopsis requires a capacity for redox regulation of the larger Rubisco activase isoform. Proc Natl Acad Sci USA 99:3330–3334